Scientific Report 2009

Institute for Energy Research-
Safety Research and Reactor Technology (IEF-6)

Safety Research for Nuclear Reactors

Content **page**

Benchmark calculations for low enriched uranium (LEU) in coated particle structure

Ch. Pohl

Institute for Energy Research - Safety Research and Reactor Technology (IEF-6), Forschungszentrum Jülich, c.pohl@fz-juelich.de

Abstract: This article comprises contributions to a benchmark project of the Oak Ridge National Laboratory and the U.S. Nuclear Regulatory Commission to fuel elements for High Temperature Gas-cooled Reactors (HTGR) [1]. Main focus of the benchmark is to identify the performance of neutron transport codes in respect to special requirements of a HTGR as heterogeneity of fuel elements and fuel particles. First step of the benchmark is the comparison of characteristic values calculated for an infinite lattice grain model. In this model the coated particles are distributed uniformly in a certain volume. Therefore only a single heterogeneity have to be taken into account. For the second step an enhanced complexity is applied. The coated particles are distributed only in the fuel zone of pebbles of 6 cm in diameter. The pebbles are considered as uniformly distributed in an infinite lattice. For the neutron transport calculation this implies another level of heterogeneity which has to be taken into account. The calculations were accomplished with the computer code V.S.O.P.(99/05) [2] for a given power density in respect to certain burn-up conditions. Characteristic parameters were determined as k-infinity, several fractions of reaction rates and fission product densities. The preliminary comparison demonstrate a good agreement with the so far know results of the other participants of the benchmark.

Introduction

Calculating neutron flux, power and temperature distribution of nuclear systems requires reliable computer codes and nuclear data libraries. But not for all calculated systems experimental data is available to validate the results. Therefore verification with other computer codes are necessary to satisfy quality requirements of the considered simulation tool. To minimize the difficulties raised from the combination of geometry description, nuclear data and different neutron transport models benchmarks typically starts with simplified geometries. For neutron transport calculations the simplest geometry is an infinite volume with homogeneous distributed fractions of fissionable, absorbing and moderation materials. So only the nuclear data is the residual point of verification.

For the coated particle fuel structure of HTGR fuel elements the next higher level of geometrical complexity is a fraction of an infinite volume of uniformly distributed coated particles. The geometry aspect arise from the structure of the coated particles and reflects a heterogeneity of the fuel distribution. The neutron transport codes have to handle this heterogeneity with appropriated methods. The following level of geometrical complexity describe a fraction of an idealised fuel element distribution in a pebble bed HTGR core. In coated particle point of view this reflects an additional heterogeneity which also have to be handled by the computer codes. Comparing the results of neutron transport codes using different methods of handling single and double heterogeneity are the focus of this benchmark.

Code design and fuel compositions

The calculations were done with the V.S.O.P.(99/05) code which take into account nuclear data based on the ENDFB- IV/V and JEFF 1 international nuclear data libraries. The neutron flux distribution is calculated by applying diffusion theory. For specific problems beyond the limits of diffusion theory (e.g. strong absorbers) appropriated transport calculations were done to determine reaction rate preserving equivalent cross sections. Doppler broadening of capture resonances and the self shielding of U-238, Th-232, Pu-240 and Pu-242 were calculated by the program module ZUT. For pebble bed HTGR a pebble bed flow schema can be applied.

The thermodynamic interaction of the inner and outer core with helium coolant is realised by a modified Thermix code which is included in the V.S.O.P.(99/05) program system. The pebble bed is considered as porous media with suitable parameters for flow resistance, heat conduction and capacity, etc. Fuel and moderator temperature is determined by individual fission rate, burn-up and neutron dose of characteristic fuel elements. For these fuel elements the specific radial temperature distribution is calculated by subdividing the pebble in 5 shells. The inner 3 shells cover the fuel zone with the coated particles embedded in a graphite matrix. Additional information to the V.S.O.P. code are available in the manual [2].

The considered coated particles (CP) consist of a 500 µm diameter fuel kernel and a 4 layered shell of graphite and SiC with of 0.09/0.04/0.035/0.04 mm thickness. The kernel consist UO_2 fuel with 10.4 g/cm³ at an enrichment of 8.2 % by mass. Additional information are available in the benchmark specification [1].

Results

In the first part calculations were done for a fraction of an infinite volume homogeneous filled with coated particles. For the considered cubical volume of 4.36351e-3 cm³ a white boundary condition, a CP packing fraction of 9.043 % and a fixed temperature of

293.6 K for fuel and moderator is assumed. To compare the different models k-infinity and characteristic ratios as fast-to-thermal capture rate of U-238 (ρ^{238}), fast-to-thermal fission rate of U-235 (δ^{235}), fission rate of U-238 to U-235 (δ^{238}) and U-238 capture to U-235 fission rate (c/f^{235}) were determined. The results are given in Tab. 1 for different burn-ups.

Table 1: Results for infinite lattice grain model

burn-up MWd/kgHM	k-inf	ρ^{238}	δ^{235}	δ^{238} *1e-3	c/f^{235}
0	1.3605	9.44	0.159	5.92	0.431
0.5	1.3024	9.86	0.166	6.21	0.449
5	1.2690	10.3	0.174	6.88	0.496
10	1.2348	10.7	0.181	7.65	0.549
20	1.1625	11.5	0.194	9.47	0.677
40	1.0516	12.6	0.212	13.9	0.989
80	0.9159	13.3	0.223	28.4	2.03
120	0.8242	13.0	0.216	60.8	4.37

The second part of the benchmark comprise calculations of a pebble bed to take into account the double heterogeneity. A cubical fraction of an infinite pebble bed of 216 cm³ is assumed with a pebble packing fraction of 52.36 %. The results are given in Tab. 2.

Table 2: Results for pebble bed model

burn-up MWd/kgHM	k-inf	ρ^{238}	δ^{235} *1e-2	δ^{238} *1e-3	c/f^{235}
0	1.5105	5.79	8.28	3.09	0.296
0.5	1.4513	5.99	8.61	3.23	0.306
5	1.4225	6.00	8.63	3.45	0.328
10	1.3958	5.96	8.56	3.70	0.353
20	1.3390	5.82	8.32	4.24	0.407
40	1.2237	5.33	7.56	5.62	0.552
80	0.9908	3.88	5.40	12.2	1.29
120	0.7624	2.71	3.71	6.86	7.98

The results show significant differences at absolute values and behaviour between the two geometry models. While e.g. ρ^{238} and δ^{235} in the grain model increase nearly continuously up to high burn-ups for the pebble bed model they decrease. This is caused by the higher moderator mass in the pebble bed because the fuel zone is covered by additional graphite layer. The neutrons therefore have a higher chance of being scattered out of the resonance energy range by moderator atoms.
A preliminary comparison of the calculated k-infinity to results of another participant of the collaboration [3] are presented in Fig. 1. For both models a good agreement can be observed for the calculated k-infinity. The remaining differences arise partly from different data libraries used in the neutron transport calculation.

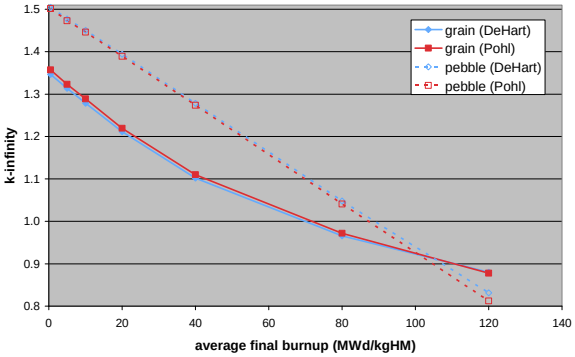

Figure 1: Comparison of k-infinity for infinite grain and pebble bed model

Summary

Characteristic parameters were calculated for two different geometry models described in the benchmark specification. The two models are intended to compare neutron transport codes in respect to the methods of handling the heterogeneities of fuel compositions. The considered parameters as k-infinity, the number density of selected fission products and different ratios of fission and capture rates characterise the considered fuel-moderator-system.
For both, the grain model (single heterogeneity) and the pebble bed model (double heterogeneity) preliminary comparisons show a very good agreement for k-infinity.

Outlook

Comparison of the proposed characteristic parameters will be done with available results of other participants of the benchmark. Additionally calculations are in progress with the updated nuclear library [4] of V.S.O.P. Based on the results of the comparison further geometry models could be determined to compare the considers codes systems on a higher level.

References

[1] M. D. DeHart, A. P. Ulses, "Benchmark Specification of HTGR Fuel Element Depletion"
[2] H. J. Rütten, K. A. Haas, H. Brockmann, W. Scherer, „VSOP(99/05) Computer Code System ", Jül-4189, ISSN 0944-2952, Forschungszentrum Jülich, October 2005
[3] M. D. DeHart, private communication
[4] K. A. Haas, "Implementation of ENDF/B-VII-based Nuclear Libraries and Update of User Data Input for V.S.O.P.-Code Version99/09 ", Internal paper, Forschungszentrum Jülich , December 2009

Deep burn-up and transmutation of a mixed Plutonium/ Minor actinides fuel for a selected HTGR reference design

Ch. Pohl, J. Li, H.-J. Rütten

Institute for Energy Research - Safety Research and Reactor Technology (IEF-6), Forschungszentrum Jülich
Corresponding author: c.pohl@fz-juelich.de

Abstract: This article comprises results of equilibrium core calculations for a HTGR (high temperature gas cooled reactor) based on the PBMR reactor design with a fuel mixture of plutonium oxide fuel (first generation plutonium of a light water reactor) and minor actinides. Different aspects were investigated especially with respect to pure plutonium oxide fuel as isotope compositions of plutonium, minor actinides and fission products in the equilibrium core and the discharged fuel, temperature reactivity coefficients for different core conditions, fuel temperatures and control rod worth. Additional some safety aspects of the fuel were discussed. The results give an impression of the influence to the high plutonium burn-up by the minor actinides and the related safety aspects. Further calculations will show an optimisation to a thorium/plutonium oxide fuel and a high burn-up in relation to the safety aspects. These calculations were done as part of the PUMA project (plutonium and minor actinides management in thermal high temperature reactors) of the EU FP6 program which focus on demonstrating the full potential of HTRs to transmute/utilise Pu/MA fuel.

Introduction

The use of nuclear energy is strongly connected with plutonium and minor actinides and there influence on final high active waste disposal and the proliferation problem of weapon grade material. To minimise both aspects a promising concept is the combination of LWRs (light water reactor) and HTGR (high temperature gas cooled reactor). This gives the opportunity for deep burn-up of the resulting plutonium from LWR and a partial transmutation of plutonium and minor actinide isotopes. To investigate the range of achievable burn-up and isotope compositions with respect to high safety characteristics of the reactor design a reference design of an HTGR with typical global parameters was studied as part of the EU FP6 PUMA program [1].

Code design and fuel compositions

The considered PUMA reference HTGR [2] is a graphite moderated helium cooled pebble bed design with an annular core of 1x11 m, a central moderator of 2 m in diameter and a thermal power of 400 MW, based on the PBMR reactor design. For the pebble bed a simplified 5 channel flow scheme is assumed without a cone at the lower end of the core. The helium cooling system is configured with 90 bar coolant system pressure, 192.7 kg/s mass flow, 500 °C inlet and 900 °C outlet temperature. Coolant bypass flows were not taken into account. Based on previous calculations to pure plutonium fuel (annular scientific report 2008) a fuel mixture of plutonium oxide and minor actinides (MA) is considered (Tab. 1). This isotope fraction is motivated by the fact that reprocessing of plutonium will extract also a certain amount of minor actinides. To see the influence of 11% MA to the final burn-up of plutonium appropriate calculations were conducted. The result are presented in this paper. A total heavy metal load of 2 g for the standard 6 cm in diameter pebbles is assumed. The equilibrium core condition were achieved for a residence time of the pebbles in the core of 974 days

Table 1: Isotope fractions of the initial fuel

Pu-238	2.90	Np-237	6.80
Pu-239	49.50	Am-241	2.80
Pu-240	23.00	Am-242m	0.02
Pu-241	8.80	Am-243	1.40
Pu-242	4.90		

Results

In contrast to pure plutonium fuel the thermal neutron flux distribution of the equilibrium core show a lower peak value and a more homogeneous distribution in axial direction but still have strong gradients to the inner and outer reflector (Fig. 1). The reduced maximum of the thermal flux results in a smaller relative power density maximum of about 2.75 in contrast to 3.0 for pure plutonium (Fig. 2).

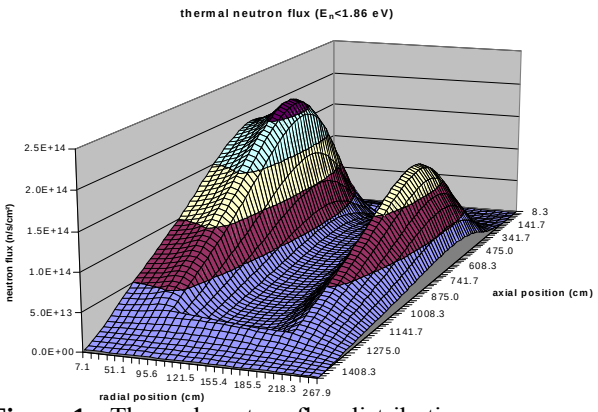

Figure 1: Thermal neutron flux distribution

The maximum pebble bed surface temperature for the equilibrium core is with 965 °C in similar range to pure

plutonium (949°C) but the maximum fuel temperature is significantly lower (1175 °C) than for pure Pu (1374°C). This is induced by the lower mass of fissionable material per pebble which produce only 3.2 kW / pebble (5.2 kW / pebble for pure Pu). Because of the higher initial amount of neutron absorbing isotopes a higher fraction of fissionable plutonium isotopes is compensated which results in a 36 % lower but still high average final burn-up of 431 GWd/tHM. Based on this lower final burn-up the overall plutonium mass is reduced only by 48 % down to average 0.922 g Pu / pebble with an isotope composition of 12.86 % Pu-238, 13.91 % Pu-239, 29.27 % Pu-240, 27.46 % Pu-241 and 16.49 % Pu-242. The total amount of minor actinides is only slightly reduced down to 0.205 g / pebble. In particular half of the mass of Np-237 is transmutated while the mass of Am-243 is doubled in the discharged fuel.

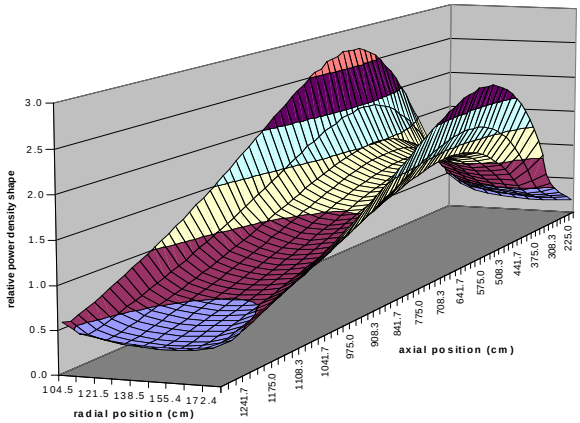

Figure 2: Power density distribution

At equilibrium condition the core contains an amount of 668.5 kg heavy metal isotopes which consists of 94 kg of other actinides, mainly the initial isotopes Np-237, Am-241 and Am-243 together with Cm-244. Additionally 36.3 kg of high absorbing fission products are in the core which is lower then for pure plutonium fuel because of the reduced burn-up. The pebbles were refilled 6 times and then discharged with a 58 % higher rate of 463.5 pebbles per day than for pure plutonium. This implies a load of 825 g and a discharge of 427.3 g of plutonium isotopes per day.

Safety aspects

For the pure plutonium fuel a temperature reactivity behaviour was observed which was not satisfying because of the positive temperature coefficient for the considered core conditions HFP (hot full power), HZP (hot zero power) and CZP (cold zero power). Because of the additional resonance absorption of the actinides in the considered fuel mixture better which means lower temperature reactivity coefficients α can be observed. The coefficients for HFP core α = -4.0867 pcm/K and for HZP α = -0.1875 pcm/K are promising because they are negative. For the CZP core the coefficient α = 9.5814 pcm/K remains positive. As expected the coefficients show better values compared to a pure plutonium fuel but still need to be improved to satisfy the requested safety requirement in particular for CZP core condition.

Summary

These calculations present the influence of minor actinides exemplarily for one initial fuel composition. The final average burn-up is reduces by 36 % to 431 MWd/kgHM compared to pure plutonium fuel. Only 48 % of the initial plutonium are burned. The initial amount of the minor actinides is only slightly reduced while the isotope fractions are significantly changed in the discharged fuel. In particular for Np-237 the initial mass is halved while for Am-243 the initial mass is doubled. Because of the epithermal resonances of some of the actinides the temperature reactivity coefficient is better than for pure plutonium fuel. For HFP and HZP core condition temperature reactivity coefficient is negative only for CZP core condition it is still positive.

Outlook

Additional calculations should be done to identify the influence of the individual minor actinide isotopes to the temperature reactivity coefficient. To evaluate the change of mass and isotope composition of the minor actinides in respect to radiotoxity appropriate investigations are required.

Acknowledgement

The work presented in this article was partly funded by the European 6th Framework Programme under contract no. 036457.

References

[1] EU FP6 project, Contract Number: 036457
[2] EU FP6 project PUMA, contribution D121

Deep burn-up of a mixed Plutonium/Thorium fuel for a selected HTGR reference design

Ch. Pohl, J. Li, H.-J. Rütten

Institute for Energy Research - Safety Research and Reactor Technology (IEF-6), Forschungszentrum Jülich
Corresponding author: c.pohl@fz-juelich.de

Abstract: This article comprises results of equilibrium core calculations for a simplified HTGR (high temperature gas cooled reactor) based on the PBMR reactor design with a fuel mixture of plutonium oxide fuel (first generation plutonium of a light water reactor) and different fractions of thorium. Several aspects were investigated especially with respect to pure plutonium oxide fuel as changes of the isotope compositions of plutonium in the discharged fuel, kernel size effects, total and individual temperature reactivity coefficients for different core conditions and variations of the final plutonium burn-up. Additional some safety aspects of the fuel were discussed. The results give an impression of the influence to the high plutonium burn-up by different thorium loads and the related safety aspects. These calculations were done as part of the PUMA project (plutonium and minor actinides management in thermal high temperature reactors) of the EU FP6 program which focus on demonstrating the full potential of HTRs to transmute/utilise Pu/MA fuel.

Introduction

The use of plutonium in nuclear energy production is correlated with measures to compensate the effects raising from the thermal and epithermal fission resonances of some of the plutonium isotopes. Usually this is done by adding a certain amount of uranium (U-235 and U-238) to the plutonium but this results in the production of new plutonium and minor actinides via neutron absorption in U-238. Another option would be the use of thorium instead of uranium. This have significant advantages (e.g. significantly reduces production of plutonium and minor actinides, higher temperature resistance) but also some disadvantages (e.g. lower resonance absorption than uranium, modification of the processing/reprocessing processes of the fuel). To investigate the opportunities of plutonium / thorium fuel compositions the achievable burn-up with respect to high safety characteristics of the reactor design a reference design of an HTGR with typical global parameters was studied as part of the EU FP6 PUMA program [1].

Code design and fuel compositions

The considered PUMA reference HTGR [2] is a graphite moderated helium cooled pebble bed design with an annular core of 1x11 m, a central moderator of 2 m in diameter and a thermal power of 400 MW, based on the PBMR reactor design. For the pebble bed a simplified 5 channel flow scheme is assumed without a cone at the lower end of the core. The helium cooling system is configured with 90 bar coolant system pressure, 192.7 kg/s mass flow, 500 °C inlet and 900 °C outlet temperature. Coolant bypass flows were not taken into account. Based on previous calculations to pure plutonium fuel [3] fuel mixtures of plutonium oxide (2.59 % Pu-238, 53.85 % Pu-239, 23.66 % Pu-240, 13.13 % Pu-241 and 6.78 % Pu-242) and thorium oxide with different mass fractions were considered (Tab. 1).

Table 1: Investigated Pu/Th loads of the initial fuel compositions

mass Pu (g/pebble)	mass Th (g/pebble)
1	1
1	2
2	2.5
2	7

The selected fuel loads allow the comparison to previous calculations for 2 g of pure plutonium [3] and reflect a first step in optimisation of Pu/Th fuel. The effects on flux distribution, burn-up and safety related aspects as temperature reactivity coefficient are presented in this paper.
Initial calculations were done for 2 g pure plutonium and two different coated particle sizes (∅ = 0.2 mm, 0.5 mm) to identify their influences on burn-up and temperature reactivity coefficient. For smaller particles it can be observed an improvement for both aspects (Tab. 2). On the other hand calculations to thorium fuel in the past are done for the larger coated particle size. The following calculations therefore were done for the larger particles to allow the comparison to previous results and to remain conservative with respect to safety aspects.

Table 2: Comparison of different coated particle size Investigated Pu/Th loads of the initial fuel compositions

	ø = 0.2 mm	ø = 0.5 mm
burn-up (MWd/kgHM)	674	650
α (pcm/K) for HFP	-2.9883	-2.6608
α (pcm/K) for HZP	1.4708	3.6271
α (pcm/K) for CZP	11.7567	14.1181

Results

With an additional amount of thorium in the fuel the moderation ratio changes and the distribution of the thermal flux becomes more homogeneous in radial (Fig. 1) and axial direction (Fig. 2).

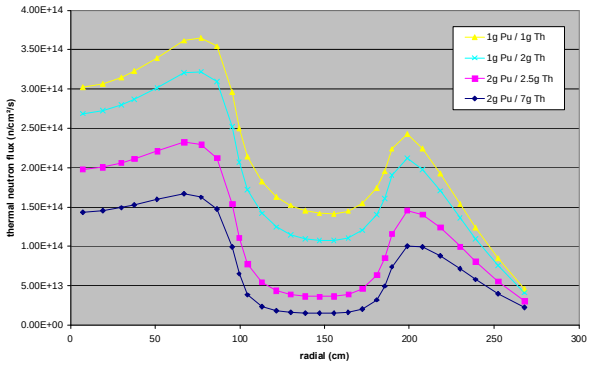

Figure 1: Radial thermal neutron flux distribution

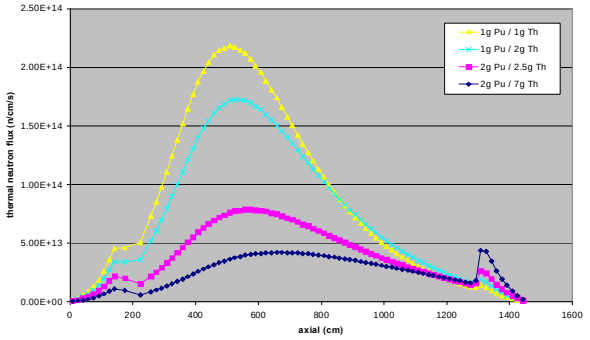

Figure 2: Axial thermal neutron flux distribution

As an advantage this directly reduce the hot spots in the inner and outer reflector and also peak power density and maximum fuel temperature (Tab. 3). But the additional amount of neutron absorbing material capture neutron which otherwise could initiate new fission reactions. Therefore a reduction of the final burn-up is expected.

Table 3: Parameter for different fuel compositions

fuel (Pu/Th)	burn-up (MWd/kgHM)	power density (W/cm³)	T_{max} (°C)
1/1	332.38	12.70	1396
1/2	222.95	11.86	1301
2/2.5	284.62	11.65	1283
2/7	51.43	10.66	1124

Beside the overall burn-up which is normalized to the total initial heavy metal mass the specific plutonium burn-up can be calculated which is normalized to the initial plutonium mass. This value represents the amount of fissioned or transmutated plutonium. Surprisingly a small amount of thorium doesn't affect this value very much, only a higher amount of thorium show the expected reduction of the final burn-up (Tab. 4).

Table 4: Plutonium specific burn-up and mass reduction (discharged/charged)

fuel (Pu/Th)	Pu specific burn-up (MWd/kgPu)	Pu-239/241 mass reduction (%)
1/1	649	99.38 / 61.76
1/2	642	99.05 / 54.15
2/2.5	614	97.24 / 36.59
2/7	226	52.66 / -31.08

So it seem feasible to find a optimised composition of plutonium and thorium with still high plutonium burn-up with a sufficient safety behaviour.

Safety aspects

Combining the plutonium fuel with a resonance absorber as thorium will result in a improvement of the temperature reactivity coefficient because of the Doppler broadening of the resonances at higher temperatures. The total coefficients for the investigated fuel composition are presented in Tab. 5 for the considered core conditions HFP (hot full power), HZP (hot zero power) and CZP (cold zero power). But additional to the total thorium mass the corresponding plutonium mass also influence the coefficient. And in a surprising way because for a nearly constant amount of thorium (≈ 2 g/FE) the coefficient increase for a reduced plutonium mass.

Table 5: Total temperature reactivity coefficient for different core conditions

fuel (Pu/Th)	α_{total} HFP (pcm/K)	α_{total} HZP (pcm/K)	α_{total} CZP (pcm/K)
1/1	0.20	8.27	18.11
1/2	-0.90	5.92	16.07
2/2.5	-3.38	0.76	9.94
2/7	-4.51	-2.09	4.71

Several effects are combined in this situation as varying self shielding effects of plutonium and thorium, change of the moderation ratio or the neutron flux spectra. Therefore to identify the main reason additional systemic calculations are needed with variations of total heavy metal load, heavy metal fraction and plutonium isotope fraction.

If we look in detail to the reactivity coefficient we find for the considered fuel compositions a maximum behaviour for the moderator coefficient which strongly influence the total coefficient in particular at low temperature (Fig. 3). This seems to be caused by the fractions of Pu-239, Pu-240 and Pu-241 in combination with the shift of the thermal neutron spectra at varying moderator temperature. For a higher load of thorium this maximum will be suppressed but for the aimed low thorium fraction the individual reasons for this behaviour should be identified and if possible reduced.

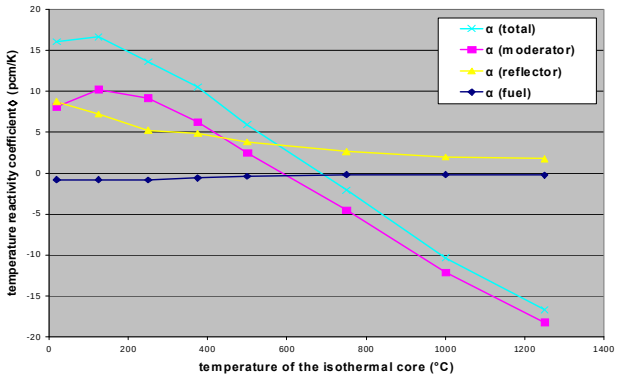

Figure 3: Individual temperature reactivity coefficients for a fuel load of 1 g Pu and 2 g Th in an isothermal core

Also in respect to an accidental water ingress the fuel compositions show significant differences. For 2 g of pure plutonium per fuel element the core is under moderated. Therefore an increase of moderator material in the core result in an strong increase of reactivity. For a smaller amount of plutonium (1 g/FE) his effect is much lower because the system is only slightly under moderated. With an additional amount of thorium the moderation ration becomes worse. But again for a small amount of thorium only a limited increase of reactivity is observable (Fig. 4).

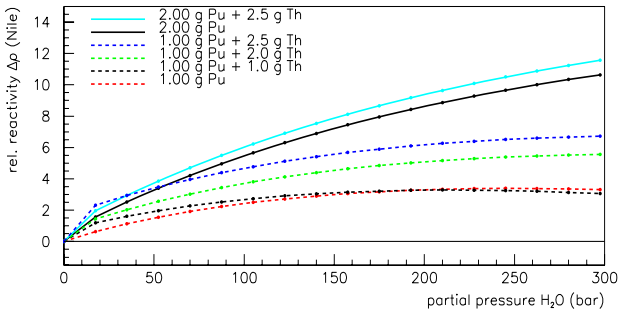

Figure 4: Relative change of reactivity for different fuel compositions

In contrast to the temperature reactivity coefficient at water ingress a better safety behaviour can be achieved with a lower plutonium load of the fuel element. Additional calculations are needed to find a optimal heavy metal load which satisfies both safety aspects.

Summary

In this paper results are presented for different heavy metal loads of plutonium/thorium mixtures which offer ideas for optimising a plutonium-based fuel for a pebble bed HTR. A optimised fuel should combine satisfying safety behaviour with a high level plutonium burn-up. It was shown that in particular for a small amounts of thorium a deep plutonium burn-up can be achieved with improved safety behaviour as reduced hot spots in the reflector, lowered temperature reactivity coefficients or limited reactivity increase at water ingress. Based on this results systemic calculation can be done to find a fuel composition which not only improve but satisfy safety requirements.

A small amount of thorium also result in a maximum behaviour of the moderator reactivity coefficient which strongly influence the total reactivity coefficient. Ideas to reduce this maximum were discussed but have to be verified with additional calculations.

Outlook

Additional systematic calculation should be done to different heavy metal loads and isotope fractions of plutonium and thorium to find a optimum fuel composition. Also variations of the initial plutonium isotope composition would be useful to determine the main reason of the moderator reactivity coefficient. For a optimised fuel composition the influence of certain amounts of minor actinides should be investigated regarding burn-up of plutonium and minor actinides and changes/improvement of the safety behaviour.

Acknowledgement

The work presented in this article was partly funded by the European 6th Framework Programme, under contract no. 036457.

References

[1] EU FP6 project, Contract Number: 036457

[2] EU FP6 project PUMA, contribution D121

[3] Forschungszentrum Jülich, annual scientific report 2008

Generic Containment – A first step in bringing nuclear accident simulation to a common level

S. Kelm[1], H.-J. Allelein[1], Ph. Broxtermann[2], S. Krajewski[2]
[1] *Institute for Energy Research - Safety Research and Reactor Technology (IEF-6), Forschungszentrum Jülich*
[2]*Institute for Reactor Safety and Reactor Technology, RWTH University of Aachen*
Corresponding author: s.kelm@fz-juelich.de

Abstract: In the case of a severe accident with and without failure of the reactor pressure vessel, the containment is the ultimate barrier to the environment. As a result there is the need to have and enhance reliable simulation tools in order to describe containment thermal hydraulics, including hydrogen distribution, the different hydrogen combustion regimes, their impact on containment structures and measures to prevent (severe) combustion processes or, at least, to mitigate their consequences with accident management measures like passive autocatalytic recombiners. One outcome of the ISP-47 (TOSQAN, MISTRA, THAI) activity [1] was the recommendation to elaborate a generic containment including all important components. This generic containment is developed in the frame of the European Network of Excellence SARNET2 (Severe Accident Research Network) under lead of JÜLICH and will help to rate analyses being performed with different lumped parameter models as well as with CFD codes. Moreover, it can serve as a basis for testing new model developments on a commonly available and accepted basis on plant scale.

Objectives

In the frame of the Network of Excellence SARNET2, 13 European organisations (Tab. 1) cooperate within the work package 7.3 'Containment – Bringing Research into Application' on the task 'Generic Containment' coordinated by JÜLICH. The proposed code-to-code comparison based on the generic containment nodalisation will consist of several runs with increasing complexity, e.g. longer and more complex accident scenarios or additional countermeasures.

Results

The initial benchmark exercise (run0) [2] is related to the following objectives:

- Preparation of input decks and a first calculation
- Assessment of transferability between the codes
- Comparison of the results, verification of input decks and first comparison of containment thermal hydraulics

In order to provide a basis for clear differentiation of input errors and different models, a simple scenario, namely the in-vessel phase of a small break loss of coolant accident (SB-LOCA) with loss of secondary heat sink, is considered. For simplifying this case in the first step only the containment thermal hydraulics are considered. The only countermeasures which are considered are those related to the primary circuit (e.g. hydroaccumulators). The primary circuit behaviour is modelled by means of source terms for steam water and enthalpy.
The general specification and nodalisation of the generic containment, has been built on the basis of a German PWR with 1300 MW_{el}. (Fig. 1) in cooperation with the RWTH Aachen University.

The rooms and compartments of the reactor and auxiliary building have been grouped into 16 control volumes (zones) in order to generate a simple generic

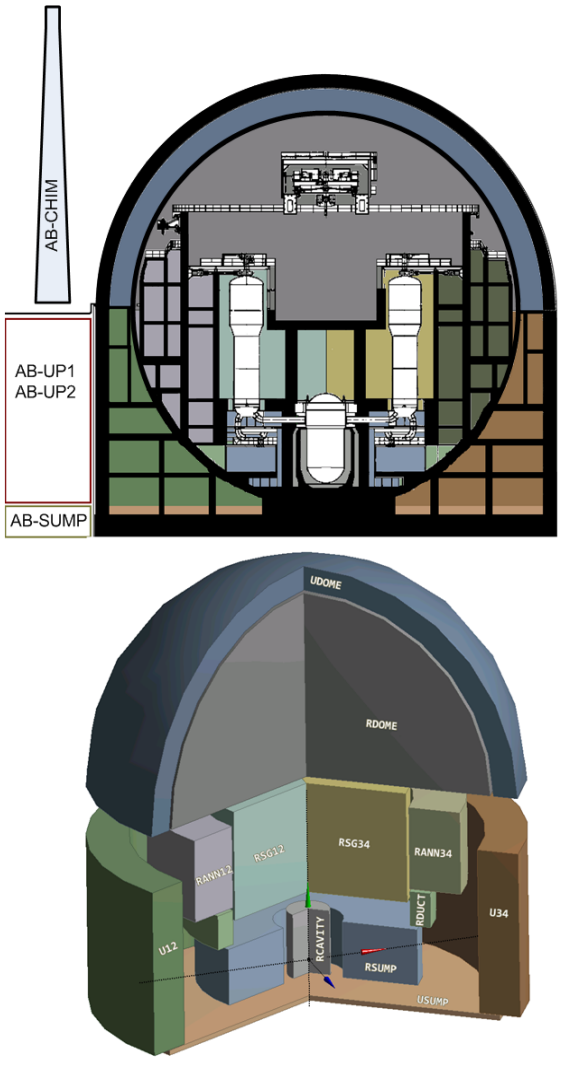

Figure 1: Generic Containment: Control volumes

Table 1: Participating organisations

Organisation	**Code**
AREVA NP, France/Germany	GOTHIC
ENEA - Ricerca sul Sistema Elettrico (ERSE), Italy	MELCOR
Forschungszentrum Karlsruhe (FZK), Germany	GASFLOW
Gesellschaft für Anlagen und Reaktorsicherheit (GRS), Germany	ASTEC, COCOSYS
Jozef Stefan Institute (JSI), Slovenia	ASTEC, CONTAIN
Institut de Radioprotection et de Sûrete Nucleaire (IRSN), France	ASTEC
Forschungszentrum Jülich (JÜLICH), Germany	COCOSYS
Nuclear Research & Consultancy Group (NRG), The Netherlands	MELCOR
Nuclear Safety Research Institute (NUBIKI), Hungary	ASTEC
Ruhr-Universität Bochum (RUB), Germany	COCOSYS
Nuclear Research Institute Rez (UJV), Czech Republic	COCOSYS, MELCOR
University of Pisa (UNIPI), Italy	ECART, MELCOR, ASTEC
VTT Technical Research Centra of Finland (VTT), Finland	APROS

nodalisation and limit model complexity. The four loops have been grouped, therefore there are two steam generator compartments R-SG12 and R-SG34 as well as the corresponding annular compartments and stair cases behind the cylindrical missile shield R-ANN12 and R-ANN34. Associated with these rooms are the compartments U-12 and U-34 within the safeguard compartments (annulus). There are common dome and sump zones R-DOME and R-SUMP within the containment and the safeguard building U-DOME and U-SUMP. The reactor cavity R-CAVITY as well as the pipe duct R-DUCT is represented by means of a single zone, respectively. In order to take the design leakage from the inner steel shell to the safeguard compartments into account, there is a connection to the lower nuclear auxiliary building AB-SUMP. Gas can distribute within the two compartments AB-UP1 & 2, leak or be vented by the exhaust chimney AB-CHIM to the surrounding environment ENVIRON. Also real structures and flow paths have been merged in order to limit model complexity. The generic containment zones are connected by means of single atmospheric (gas) and drain (fluid) junctions. In order to reduce complexity doors, rupture discs and pressure relief flaps have been joined and are considered in a simple way by means of a rupture disc model. Figure 2 shows the connection of the control volumes by means of junctions.

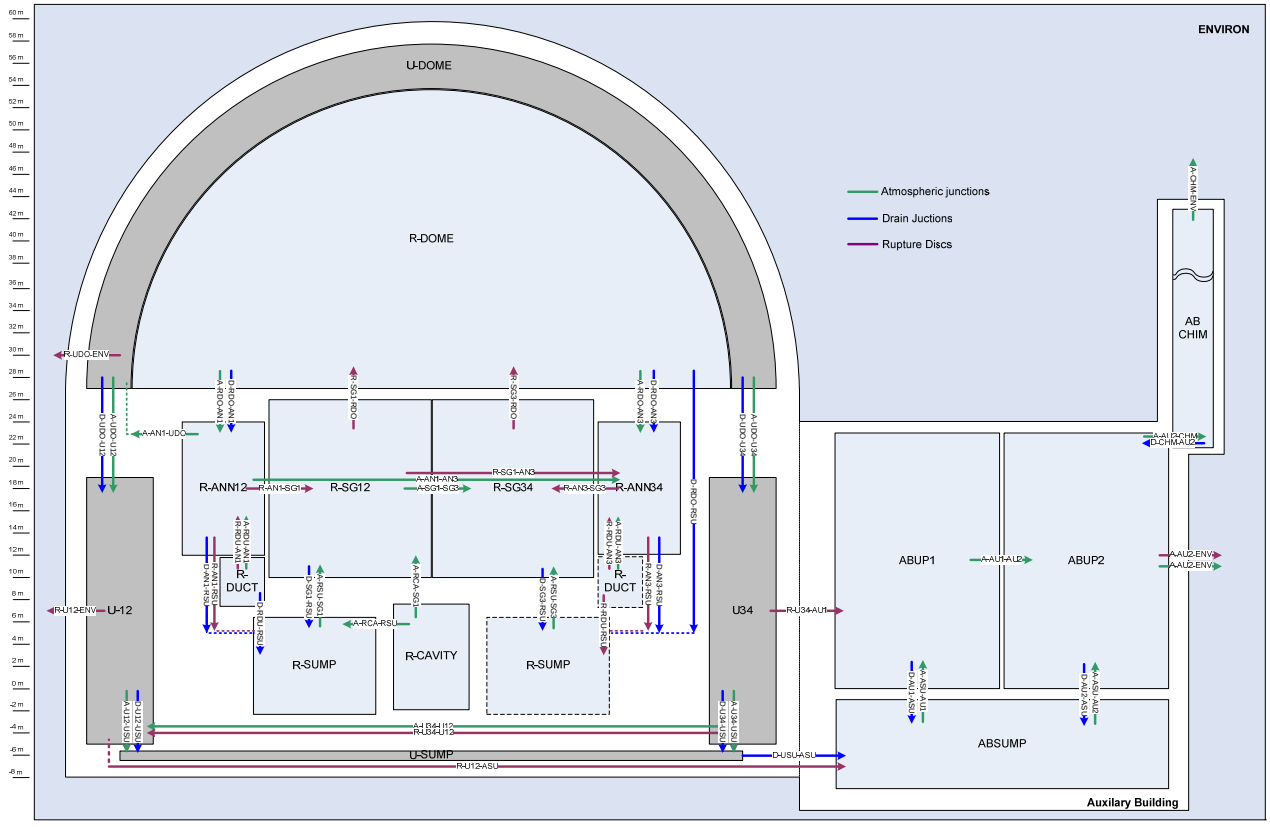

Figure 2: Generic Containment: Connection of control volumes by means of junctions

Summary & Outlook

In order to establish a commonly available and accepted basis for the comparison of nuclear accident codes in the frame of SARNET-2 a generic containment nodalisation has been built and proposed in cooperation with the RWTH Aachen University. In the frame of a first code-to-code comparison especially the input preparation and verification as well as the transferability between the different codes are addressed. Feedback by participants took the requirements of different codes and models into account and resulted in a revised specification. Results of the initial benchmark run are expected for May 2010.

References

[1] H.-J. Allelein et al.: *International Standard Problem ISP-47 on containment thermal hydraulics – Final Report*, NEA/CSNI/R(2007)10, 2007

[2] H.-J. Allelein, S. Kelm, Ph. Broxtermann, S. Krajewski: *Proposal for a generic containment & specifications for the code-to-code comparison – run0*, Report NoE SARNET2, 2009.

Integration of experimental facilities in the European network of hydrogen safety (HySafe)

E.-A. Reinecke

Institute for Energy Research - Safety Research and Reactor Technology (IEF-6), Forschungszentrum Jülich, e.reinecke@fz-juelich.de

Abstract: In the area of hydrogen safety, research facilities are essential for the experimental investigation of relevant phenomena, for testing devices and safety concepts as well as for the generation of validation data for the various numerical codes and models. In the framework of the European HySafe Network of Excellence (NoE), the activity 'Integration of Experimental Facilities (IEF)' - coordinated by JÜLICH - has provided basic support for jointly performed experimental work. Even beyond the funding period of the NoE HySafe in the 6th Framework Program, IEF represents a long lasting effort for reaching sustainable integration of the experimental research capacities and expertise of the partners from different research fields in the frame of the new established International Association HySafe. In order to achieve a high standard in the quality of experimental data provided by the partners, emphasis was put on the know-how transfer between the partners. On the one hand, a documentation of the experimental capacities has been prepared and analysed. On the other hand, a wiki-based communication platform has been established supported by biannual workshops covering topics from measurement technologies to safety issues. Based on the partners' contributions, a working document on best practice including the joint experimental knowledge of all partners with regard to experimental set-ups and instrumentation was created.

Objectives

The introduction and commercialisation of hydrogen as an energy carrier of the future makes great demands on all aspects of safety. In the frame of the 6th European Framework Program, the HySafe Network of Excellence (NoE) has been aiming at the integration of the European research activities in the area of hydrogen safety and to disseminate the knowledge and achievements. 24 partners from such different fields as automotive industry, nuclear safety research, or risk assessment consultancy have contributed to this effort [1].

All activities and projects of HySafe have been organised in the four clusters 'Basic research', 'Risk management', 'Dissemination' and 'Management'. Among these, the work of the cluster 'Basic Research' mainly consists of knowledge consolidation providing a well structured hardware and software infrastructure for the network. In this way, the cluster has supported e.g. the internal projects InsHyde (Releases in confined and partially confined spaces) and HyTunnel (Safe tunnels for hydrogen vehicles). The capability of adequately assessing different accident scenarios has been demonstrated in a set of numerical benchmark studies. For validation purposes, these numerical studies are based on high quality experimental data, especially with regard to the increasing capabilities of high resolution CFD (Computational Fluid Dynamics) tools.

Consequently, the objectives of the activity Integration of Experimental Facilities (IEF) coordinated by JÜLICH were to enable the HySafe network to jointly perform high level experimental research by supporting the partners' development of excellence, broadening the fields of experience, and at the same time enhancing the communication and knowledge base.

At the beginning of HySafe, the IEF partners were operating numerous test facilities in national or international projects for diverse research tasks reaching from material research in laboratory scale to full scale explosion studies. Consequently, there was a need to identify the partners' best expertise, potentially overlapping activities but also possible gaps. Furthermore, the exchange of expertise and know-how between the partners has been regarded as one of the keys to provide high quality experimental data.

Results

The experimental activities in the field of hydrogen safety in Europe mainly originate from two areas: On the one hand, hydrogen safety research has developed from safety investigations for natural gas applications. On the other hand, in the field of nuclear technology, hydrogen is a safety issue in 'severe accident' research since more than 20 years. In the frame of IEF, 15 partners from both research fields have been contributing with their specific expertise. Furthermore, the partners originate from private and governmental research, industry and universities with certain historical differences in the methodologies and approaches for addressing safety issues.

- Bundesanstalt für Materialforschung und -prüfung (BAM), Germany
- Commissariat à l'Energie Atomique (CEA), France
- EnergieTechnologie (ET), Germany
- Fraunhofer Institut Chemische Technologie (Fh-ICT), Germany
- Forschungszentrum Juelich GmbH (FZJ), Germany
- Forschungszentrum Karlsruhe GmbH (FZK), Germany

- GexCon AS (GexCon), Norway
- The United Kingdom's Health and Safety Laboratory (HSL), United Kingdom
- Fundación INASMET-Tecnalia (INASMET), Spain
- Institut National de l'Environnement Industriel et des Risques (INERIS), France
- The EC's Joint Research Centre - Institute for Energy (JRC), Netherlands
- Russian Research Center Kurchatov Institute (KI), Russia
- The Netherlands Organisation for Applied Scientific Research (TNO), Netherlands
- University of Pisa – DIMNP (UNIPI), Italy
- Warsaw University of Technology (WUT), Poland

The in total 109 experimental facilities available at the IEF partners spread over a wide range of scales and applications with regard to hydrogen safety research. Table 1 gives a brief - however rough - summary of the specific experimental orientation and capacities of the partners.

In the frame of the network activities, the total of 109 facilities has been categorised in order to identify specific expertise, map research needs with research possibilities in order to identify gaps, and enhance the presentation of the facilities.

As a basis for the categorisation, the phenomena and parameters related to accidental events and possible consequences introduced in the Phenomena Identification and Ranking Table (PIRT) have been used. The PIRT exercise had been performed in the framework of HySafe with the objective of identifying and prioritising R&D needs in the area of hydrogen safety. The main categories characterising the main fields of application of the experimental facilities are:

- Gaseous release
  Gaseous releases of hydrogen starting from small release rates resulting from permeation up to full bore rupture (pipe) or full vessel rupture.
- Dispersion
  Numerous phenomena are related to hydrogen dispersion, e.g. the influence of the environmental conditions and obstacles on flow patterns, heat transfer and the possible formation of stratifications. The effects of natural and forced ventilation as well as buoyancy effects require substantial experimental research for reliable predictions of the distribution of hydrogen after an accidental release.
- Ignition
  Ignition of flammable hydrogen/air mixtures may occur due to numerous mechanisms. Besides auto-ignition, shock, static electricity, radiation, hot surfaces, hot jet, etc. may cause ignition.
- Combustion/explosion
  Studies on hydrogen combustion and explosion is the category with the largest number of facilities available in IEF, reflecting the complexity of the topic from the scientific point of view, taking into account different flame types (laminar, cellular, wrinkled, standing, self-turbulising), the propagation of flames (e.g. acceleration and deceleration due to obstacles or concentration gradients) and the possible transition from deflagration to detonation (DDT).

Table 1. Summary of the test facilities operated by the IEF partners

Partner	**Experimental facilities**
BAM	Test facilities for material testing, sensor testing and gas explosion experiments
CEA	Test facilities for gas release and distribution experiments
ET	Cryogenic hydrogen test facilities (up to 40 MPa), high-pressure hydrogen test facilities (up to 100 MPa), hydraulic burst tests, leak/permeation measurement, material/embrittlement tests (100 MPa, 300°C)
Fh-ICT	Test facilities for H_2 deflagration and detonation experiments
FZJ	Small-scale test facilities for studying hydrogen mitigation devices
FZK	Test facilities to study H_2 explosion phenomena and H_2 distribution
GexCon	Small and large-scale test facilities for explosion experiments
HSL	Fire and explosion test facilities, facilities for assessing dispersion and mixing of both gaseous and two-phase flashing flows, facilities for ignition research, facilities for jet and pool fire testing, impact test facilities including air cannon and impact test track
TECNALIA-INASMET	Small scale facilities for studying the effect of hydrogen on materials behavior
INERIS	Facilities to study hydrogen combustion propagation in industrial pipes, unconfined jet release of hydrogen (free or impinged jet), confined hydrogen explosion and explosion venting, slow release of hydrogen in confined spaces (garage), and pressurized tank and liquid tanks testing
JRC	Compressed gas hydrogen tank testing facility, solid state storage facility and hydrogen sensor testing facility
KI	Several combustion tubes, special vented tubes, scaled multi-compartment facilities for FA and DDT studies, spray facility for experiments with liquid fuel, bunker facility
TNO	Test facilities for combustion and explosion experiments, IBBC Bunker for (semi)confined explosions, rigs for testing confined explosions, detonation tube facilities, explosion facility (e.g. for testing rocket engines)
UNIPI	Large-scale CVE facility (30 m³) for confined vented explosion experiments
WUT	Detonation tube facility for studies of gaseous detonations

- Liquid release and explosion of liquid storage
  Experimental work on liquid hydrogen (LH2) wasn't prominently represented in the initial IEF consortium. In 2007, the consortium was enhanced by company ET which is operating several facilities on LH2 As an example, in the LH2 vacuum insulation rupture rig the behaviour of a LH2-car tank under spontaneous rupture of vacuum insulation is studied in full scale by means of high speed camera recording.
- Mitigation
  The category 'mitigation' includes the prevention of combustion processes – e.g. by means of natural or forced convection, inerting, recombiners – preventive ignition, venting of deflagration, up to blast wave-protective wall-interaction.
- Equipment and device testing
  The category 'Equipment and device testing' includes the fields
  - performance tests: sensors, igniters, recombiners
  - storage tests
  - material tests
  - impact tests: explosion, thermal, mechanical, dynamic pressure.

For the total of 109 facilities, fact sheets have been provided by the IEF partners containing basic technical information on the facilities. An on-line version has been implemented in the HySafe web page as well. A similar compilation of fact sheets has been performed for the instrumentation of the facilities.

While the compilation of experimental facilities descriptions provides an overview of the experimental capacities of the IEF partners, the exchange of expertise and know-how is one of the keys to achieve high quality experimental work. Consequently, a series of workshops was initiated and a common internet communication tool has been established as part of the HySafe web page.

In order to ensure a common quality standard, a series of biannual workshops on topics related to measurement techniques and experimental work was started in the second year of HySafe. The general aim of the IEF workshops was to become acquainted with the partners' activities, to share knowledge in the field of experimental work and to support jointly planned and performed experiments. In this respect, these workshops served for improving and maintaining the quality of experimental work and supported the integration process as well. The workshops included presentations by the IEF partners related to the workshop topic, visits of experimental facilities, and presentations and discussions on planned and performed experiments.

A total of 8 well received workshops has been jointly organised covering topics from measurement technologies to safety issues (Table 2). Based on the contents presented by the partners, a working document on best practice including the joint experimental knowledge of all partners with regard to experiments and instrumentation was created. Preserving the character of a working document, it was implemented in the IEF wiki website which was set up in order to provide an internal communication platform (not publicly accessible), including information e.g. on

- workshop planning
- overview of on-going experiments
- status of internal projects
- access to internal documents

Table 2. History of IEF workshops

Date / location	**Topic**
5-6 July, 2005, Fh-ICT, Germany	Hydrogen concentration measurements
16-17 Nov., 2005, INERIS, France	Temperature and heat flux measurements
5-6 April, 2006, HSL, UK	Velocity measurements in gases and flames
10-11 Oct., 2006, CEA, France	Dynamic pressure measurements
12-14 Mar., 2007, ET, Germany	Data acquisition systems
25-27 Sept., 2007, WUT, Poland	Optical measurement techniques
22-24 April, 2008, FZJ, Germany	Software for data analysis and presentation
20-22 Oct., 2008, UNIPI, Italy	Safety aspects of hydrogen experiments in facilities

The implemented working document includes all presentations given at the workshops organised along the measurement techniques

- (hydrogen) concentration measurements,
- temperature measurements,
- gas velocity measurements,
- flame speed measurements,
- pressure measurements,

and the experimental tasks. The further contents includes the processing of experimental data and safety aspects of experiments with hydrogen.

Outlook

Being part of the 'Basic research' cluster, IEF has provided basic support for jointly performed experimental work in HySafe. The collection of IEF documents - including the descriptions and fact sheets of the experimental facilities and measurement techniques, and the working document on best practice – provides an excellent basis for the continuation of joint activities in the framework of the new-founded International Association HySafe.

Two activities are expected to become basic part of future activities: The series of IEF workshops and joint IEF studies on challenging measurement tasks aiming at the improvement of the know-how on specific

measurement techniques. Some partners have already expressed their interest in joint studies on mini-katharometers for hydrogen concentration measurements.

While the series of workshops has already demonstrated the readiness of the IEF partners to share knowledge in the field of experimental work, the internal studies on challenging measurement tasks will demand an even higher level of co-operation.

Acknowledgements
The IEF activities within the HySafe NoE has been partially funded by the European Commission in the 6th Framework Program.

References
[1] T. Jordan, L. Perrette, H. Paillère: HySafe - The European Network of Excellence on Hydrogen Safety, 1st International Conference on Hydrogen Safety, Pisa, Italy, September 9-10, 2005

Refactoring of the reactor dynamics code MGT as a first step towards a modular HTR code package

C. Druska, S. Kasselmann, S. Scholthaus

Institute for Energy Research - Safety Research and Reactor Technology (IEF-6), Forschungszentrum Jülich
Corresponding author: s.kasselmann@fz-juelich.de

Abstract: Refactoring is a disciplined technique for restructuring an existing body of code, altering its internal structure without changing its external behavior. It is a well known and frequently used method in the field of computer science which has proven its worth. The goals of refactorization are to increase readability, to eliminate duplicate code and to speed up the implementation of new features. Within this project, first parts of the reactor dynamics code MGT have been successfully refactored. One part is an interface program which preprocesses data from other codes to be read by MGT. As a side effect of the refactoring, the amount of code was reduced by 350 lines (14.6%) while at the same time providing extended functionality to the user. Another part which has been studied is the spectrum calculation program TiSpec. The aim of the refactoring here was to separate the data input layer from the actual algorithms. This is necessary to be able to implement a new spectrum calculation code while keeping existing input methods. To ensure the software quality and to minimize the introduction of new bugs, a version control and documentation system is used. The overall aim of this work is to build an integrated and multidisciplinary code system which is able to simulate all neutronic, thermohydraulic as well as fuel performance and release aspects of a high temperature gas cooled reactor (HTR) through the whole lifetime.

Objectives

The quality of any long-lived source code tends to degrade over time. Such systems often exhibit code duplication and global information sharing. Maintenance and expansion can become tedious, costly, and time-consuming work. One solution to this gradual software decay is refactoring [1]. A refactoring process is advisable, if the following criteria do apply for a code (excerpt):

- usage of long methods and parameter lists
- presence of duplicated or dead code parts
- presence of patterns like shotgun surgery, data clumps, temporary fields, primitive obsession,…

Special care has to be taken in case of old legacy Fortran code. Here a lot of potential problems have to be removed first (excerpt):

- implicit data types
- common blocks
- equivalence statements
- memory address calculations
- static memory allocation
- six character variable naming
- highly nested loops and logical conditions
- capitalization through the whole code
- fixed format code layout
- missing indentation

The reactor dynamics code MGT [2] is based on the former program TINTE, whose development began about 30 years ago. The 37,000 lines of code are mainly written in Fortran 77. Therefore the former authors were necessarily compelled to use few character strings for variable and subroutine names, long parameter lists and combinations of common blocks with equivalence statements. From today's point of view this kind of code has a lot of limiting aspects. The implementation of new features for example is slowed down, because new users can hardly understand the code and changes are often harming supposedly independent parts of the code. Therefore a refactoring process of MGT has been initiated.
Because a detailed knowledge about the modeled physics is mandatory to perform extensive code rearrangements, refactoring needs a cooperation of scientists and software engineers.

Results

Before the actual refactoring could be started, the code was modified with respect to recent programming standards (e.g. Fortran 90/2003). Most of the problems during this project arose due to non-compliant source code where bugs could not automatically be detected by the compiler.
Through the following refactoring, the basic code structure of MGT was drastically changed in many ways. At the same time the simulation results which have been validated over a long period of time must be reproducible. This could be guaranteed by setting up a version control and documentation system [3], where every modification of the code is tagged and cross-checked using a standardized set of input test samples. More than 400 code revisions are tagged in the version control system which is accessible through a file server by every work group member. Each of them has been checked to reproduce the results of the previous ones. Other software development groups are going to join this project with their codes, so that a first step towards

a consolidation of the so far slightly bound codes towards a HTR code package is being made.

So far several parts of MGT have been successfully refactored. One of them is the interface program between V.S.O.P. [4] and MGT. This program is needed, because both codes are using different calculation meshes and nuclide databases for example. One major issue here was to concentrate all *READ* statements which were spread over the whole file into distinct subroutines, each of them now being responsible for a dedicated file only. Problems occurred here due to interdependencies as a result of non sequential reading from different input files. Another issue was the static allocation of memory based on integer address calculation. This code has been replaced by dynamic memory allocation. After having removed all *common blocks* in favor of external *modules*, the whole code was split up into smaller subroutines applying the *ExtractMethod* refactoring strategy. As a side effect, the amount of code could be reduced by 350 lines (14.6%) while at the same time providing a better usability.

Another part of MGT which has been reviewed is the spectrum calculation program TiSpec. It calculates the critical spectrum of a bare homogeneous reactor in 43 neutron energy groups. This spectrum is then used to evaluate condensed microscopic cross-sections. The aim of the refactoring here was to separate the data input layer from the physics code. This is mandatory for the implementation of a new spectrum calculation code while keeping existing input methods. Most of the problems here occurred due to a lot of nested logical structures and *goto* statements.

As an example Fig. 1 shows a typical situation before the refactoring. The subroutine continues over several pages (not shown here), the different tasks of this subroutine are not clear from the source itself.
In Fig. 2 the same piece of code after the refactoring process is shown. The subroutine has been subdivided according to its tasks. The names are self-descriptive and underline the sequence of workflow.

Until now several thousand lines of MGT code have been updated according to recent Fortran standards and refactored with respect to the physics tasks. This modernization process should be completed before any new feature is implemented.

Outlook
The refactoring process of MGT is far from being finished. Only a part of the 35,000 lines of code have been studied in detail yet.

The overall aim of this work is to set up an integrated and multidisciplinary code system which is able to simulate all neutronic, thermohydraulic as well as fuel performance and release aspects of an HTR reactor through the whole lifetime.

```
      subroutine tispecrl (j2,kmatg,imatg,ljg,njg,lkg,nkg,
     >   libkart,fisg,satzq,satzr,satzs)

C     Subroutine TISPECRL erstellt die interne Kurz-Library fuer   !AL68
C     diesen Job.                                                  !AL68

CC    IMPLICIT REAL*8(A-H,O-Z)          ! darf hier fehlen         !AL68

      integer imatg(kmatg)
      real*4 fisg(62)
      real*4 satzq(193,kmatg)
      real*4 satzr(ljg,njg)
      real*4 satzs(lkg,nkg)
      real*4 x(193)

      CHARACTER*88  libkart(-1:njg+nkg)


      READ (J2,'(9A4,16x,3I4)') (x(I),I=1,9), NI,NJ,NK
      write (libkart(-1),'(9A4,16x,3I4)') (x(I),I=1,9), NI,NJ,NK
      READ (J2,'(7(6E12.5,/),2E12.5,/,3(6E12.5,/))') (fisg(K),K=1,62)

      DO I = 1,NI
              READ (J2,'(6A4,3X,F9.6,2E12.5)') (X(L),L=1,9)
              READ (J2,'(7(6E12.5,/),E12.5)') (X(L),L=22,107)
              IF (X(7)-1.0.GE.0) THEN
                  READ (J2,'(7(6E12.5,/),E12.5)') (X(L),L=108,193)
                  DO L = 10,21
                     X(L) = 0.0
                  END DO
              ELSE
                  DO L = 108,193
                     X(L) = 0.0
                  END DO
                  READ (J2,'(6E12.5)') (X(L),L=10,21)
              END IF
              do j=1,kmatg
                 if (imatg(j).eq.i) then
                   do l=1,193
                     satzq(l,j)=x(l)
```

Figure 1: Subroutine *tispecrl* before the refactoring process (excerpt)

```
!*******************************************************************
! builds interal compact library for this job
!
! called by StoreTispecAndTn4Data (Tispsub.f90)
!*******************************************************************
      subroutine StoreTispecData (kmatg,imatg,lrg,nrg,lsg,nsg,          &
     &                            libkart,fisg,satzq,satzr,satzs)

        use mgt_io_units, only: itispi

        implicit none

!---- variables from parameter list
        integer  (kind=4)                          :: kmatg,lrg,nrg,      &
     &                                                lsg,nsg
        integer  (kind=4), dimension(kmatg)        :: imatg
        real     (kind=4), dimension(62)           :: fisg
        real     (kind=4), dimension(193,kmatg)    :: satzq
        real     (kind=4), dimension(lrg,nrg)      :: satzr
        real     (kind=4), dimension(lsg,nsg)      :: satzs
        character(len=88), dimension(-1:nrg+nsg) :: libkart

!---- local variables
        integer(kind=4)                            :: k,l          ! loops


        call StoreHeaderData (nrg,nsg,libkart)

        call StoreEnergyData (fisg)

        call StoreXSectionData (kmatg,imatg,satzq)

        call StoreResonanceData (nrg,lrg,nsg,libkart,kmatg,imatg,satzr)

        call StoreScatteringData (nrg,lsg,nsg,libkart,kmatg,imatg,satzs)

      end subroutine StoreTispecData
```

Figure 2: Subroutine *StoreTispecData* after the refactoring process

The first step towards this HTR code package is the consolidation of the different thermohydraulics codes used today. Therefore an internal benchmark has been initiated to identify the most suitable thermohydraulics code to replace all the other thermohydraulics models actually in use.

In a second step the different spectrum calculation codes in MGT and V.S.O.P. will be replaced by the TOTMOS code [5]. Further work has to be done in the field of decay heat which actually is also calculated differently in both codes. Finally other codes like FRESCO [6] will be coupled. This would allow to calculate the fission product release for a whole reactor lifetime taking into account all kind of reactor operation modes.

References

[1] Fowler, M. (1999), Refactoring: Improving the Design of Existing Code, Addison-Wesley, 1999

[2] C. Druska, St. Kasselmann, A. Lauer (2009), Investigations of space-dependent safety-related parameters of a PBMR-like HTR in transient operating conditions applying a multi-group diffusion code, Nuclear Engineering and Design 239 (2009) 508–520

[3] Ben Collins-Sussman, Brian W. Fitzpatrick, C. Miachel Pilato (2004), Version Control with Subversion – Next Generation Open Source Version Control, O´Reilly Media, June 2004

[4] H.-J. Rütten, K.A. Haas, H.Brockmann, W. Scherer (2005), V.S.O.P. (99/05) Computer Code System– Very Superior Old Programs, JÜL-report 4189

[5] H. Brockmann, TOTMOS User Manual, (to be pusblished)

[6] H. Krohn, R. Finken (1983), FRESCO-II – Ein Rechenprogramm zur Berechnung der Spaltproduktfreisetzung aus kugelförmigen HTR-Brennelementen in Bestrahlungs- und Ausheizexperimenten, JÜL-Spez-212

Development of a XML scheme for the nuclear data input file of the reactor dynamics code MGT

S. Scholthaus, St. Kasselmann

Institute for Energy Research - Safety Research and Reactor Technology (IEF-6), Forschungszentrum Jülich
Corresponding author: s.kasselmann@fz-juelich.de

Abstract: For the simulation of high temperature nuclear reactors (HTR) a variety of input information is needed. Because the equations for neutron diffusion and heat transport are solved on a two or three dimensional grid using the finite difference approach, isotope compositions, cross sections, temperatures or decay heat data has to be provided for each so called mesh of the reactor geometry model. In the past, plain text files were used which had been extended several times due to enhanced modeling algorithms. Because of the limited amount of memory at the time of the first input file design, the input had to be modified in a way that led to heavy fragmentation, improper usage of data types and multiple meanings of variables at distinct positions in the file. The aim of the work described here was the development of a new, flexible and future proof data input concept by applying state-of-the-art technologies like XML and XSLT. Within this project, an XML scheme for the nuclear input data of the reactor dynamics code MGT has been developed. As a result, the input data now is clearly identifiable, properly encapsulated and modular arrangeable. Furthermore each piece of information is self-descriptive due to meaningful tag names. This project is the first step towards a complete XML based input description which, once developed, can also be applied to other computer codes actually being used in the institute.

Objectives

To make use of data from a file for a program like MGT [1], the data has to be provided in a certain format. Basically there are two formats available: plain text and binary. The latter one has the advantage of low storage requirements and can be read easily by a simple program. Such files are used in MGT for the purpose of data analysis. The downside that the data can not be checked without an appropriate program is of minor interest since the post-processing is fully automated and no additional user input is required.

An alternative is to use plain text files as MGT does for all of its input. The higher need of disk space for plain text files can be neglected considering the substantial advantages of this format. Because input files always contain specific information for each problem, a part of the nuclear input data for MGT has to be added manually by the user. Thus binary files are not adequate for this purpose.

The problem of the simple plain text input file actually used in MGT is, that it must exactly match a specified format. Sometimes the correct position of the data can only be achieved by counting the number of lines or columns. Also an exact number of blanks or empty lines has to be given at different locations in the file. If there is an unintended shift, for example, this can have far-reaching consequences when reading the data. Parts of the information can be lost or incorrect values for certain variables are passed to the reading program. Moreover, most of the input data is not checked for possible errors while being read. An input error can have an effect much later in the program execution. Finding such an error is very time consuming. For these reasons the new input scheme had to meet the following requirements:

- proper encapsulation of data
- increase of the readability of data
- avoidance of unused or redundant information
- conflation of related information into data objects
- order independence of different data structures
- implicit control of correct data types
- implicit control of correct data ranges
- usage of open source software libraries

The Extensible Markup Language XML [2] qualifies for all of these demands perfectly. The data is strictly encapsulated by opening and closing tags. Due to meaningful elements names, the kind of data can clearly be identified. There is no need for fixed patterns and the possibility of nested tags allows to model complex object oriented like data structures. The content is independent of the order and position within the file. Thus one has the possibility of direct access to all information. Unused and redundant (duplicate) data can be avoided, which actually has to be specified due to format reasons. Any non-compliance with respect to the XML scheme will be detected automatically before any data is passed to the program. Even more the parser points exactly to the position of error in the input file.

Results

The new format of the input file only consists of three root elements: *Header*, *Meshes* and *DecayHeat.* The element header contains basic information about the current file. Here additional information about the file is now included. Since the various data for MGT is stored in several files, this information provides the ability to easily identify related files. The number of energy groups, which will be used in the current reactor model is now limited in the range between 1 and 43, since MGT can handle at most 43 energy groups. In the original input file, these data were included in every mesh.

After the header, a list of three different kind of meshes follows. As an example, Fig. 1 shows the internal structure of the data object *ReflMesh*. While the information in the old input scheme was identified just by its position within the file, now a structured "tree" of data objects exists.

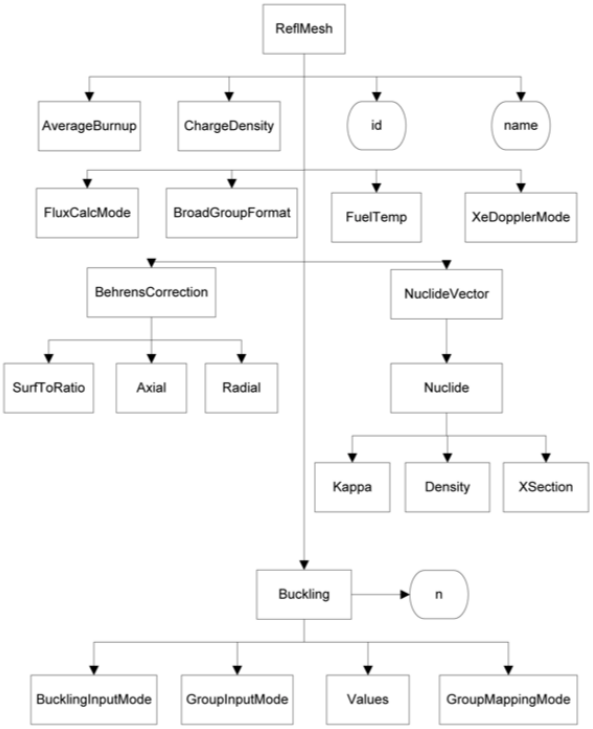

Figure 1: Structure of the XML element *ReflMesh* representing a reflector mesh in the reactor model.

The *NuclideVector* for example contains several nuclides and each nuclide has up to three different properties (see Fig. 2) but not all of them have to be specified. For each property additional restrictions can be defined like a specific valid data range or the way of data representation (e.g. scientific notation).

The last part of the file consists of the decay heat history for the actual reactor model. Fig. 3 shows the corresponding XML scheme. As can be seen, some variables are defined to be a *decimal* number, others are *integers*. Also user defined data types like *groups* can be used. They have to be specified later on in the file. There are some values like the *average power density* of the reactor or the *average final burnup*. To provide the values correctly, the unit is needed as well. Therefore the XML scheme contains comments for each variable where the correct unit is given which is expected by the program.

```
<tn4:NuclideVector>

  <tn4:Nuclide id="2" name="Pa-233" kernel="true">
    <tn4:Density>  0.80139E-14 </tn4:Density>
  </tn4:Nuclide>

  <tn4:Nuclide id="9" name="U-238">
    <tn4:Density>  0.10848E-03 </tn4:Density>
    <tn4:Kappa>    0.40000E+00 </tn4:Kappa>
  </tn4:Nuclide>

  <tn4:Nuclide id="20" name="C-12">
    <tn4:Density>  0.52624E-01 </tn4:Density>
    <tn4:Temp>     0.79247E+03 </tn4:Temp>
    <tn4:XSection> 0.38800E+01 </tn4:XSection>
  </tn4:Nuclide>

</tn4:NuclideVector>
```

Figure 2: Example of the data type *NuclideVector* with three *Nuclides* each having a different set of properties.

```
<complexType name="DecayHeat">
      <all>
       <element name="AvPowerDensity"   type="decimal"    />
       <element name="MetalContent"     type="decimal"    />
       <element name="AvFinalBurnup"    type="decimal"    />
       <element name="KernelOverheat"   type="decimal"    />
       <element name="SafetyFactor"     type="double"     />
       <element name="PrevPowerLevel"   type="integer"    />
       <element name="CalculationMode"  type="double"     />
       <element name="TimeIntervals"    type="TimeIntervals" />
      </all>
      <attribute name="ntherm" type="groups" use="required" />
      <attribute name="nfast"  type="groups" use="required" />
</complexType>
```

Figure 3: User defined XML data type for the decay heat.

More details about this new XML based input file can be found in [3].

Outlook

After the successful definition of the XML scheme, the old input scheme will be replaced by the new XML based input. Therefore an XML writer and reader has to be developed which will provide the data to a data interface in MGT. One of the candidate libraries to be used here is the Fortran XML library FoX [4]. In a first step, the data input concept of MGT will be adapted to fit into the new concept. The second step includes the programming of the XML parser. It will also be possible to translate the old input files which have accumulated over the years into the new XML design based input. This work package will be part of a bachelor thesis.

Further ideas include the visualization of the new input files via XSLT in a conventional web browser [5]. One advantage here is the possibility of linked information. For example, the created HTML document could contain a list of all core, reflector and void meshes of the reactor model which can be clicked on to directly being led to the specific mesh of interest in the file.

References

[1] C. Druska, St. Kasselmann, A. Lauer (2009), Investigations of space-dependent safety-related parameters of a PBMR-like HTR in transient operating conditions applying a multi-group diffusion code, Nuclear Engineering and Design 239 (2009) 508–520

[2] Helmut von Hoegen (2009), Einstieg in XML, Grundlagen, Praxis, Referenz, Galileo Computing, 2009, 5. aktualisierte Auflage

[3] Sarah Scholthaus (2009), Entwicklung eines XML-Schemas für die nukleare Eingabedatei der nukearen Eingabedaten des Fortranprogramms MGT, Seminarbeit, Dezember 2009

[4] Oby White, FoX – a Fortran XML library, http://uszla.me.uk/space/software/FoX

[5] Doug Tidwell (2008), XSLT – Mastering XML Transformations (2nd Edition), O´Reilly, 2008, ISBN 978-0-596-52721-1

Oxidation kinetics of innovative carbon-based materials in severe air ingress accidents in HTRs

B. Schlögl

Institute for Energy Research - Safety Research and Reactor Technology (IEF-6), Forschungszentrum Jülich, b.schloegl@fz-juelich.de

Abstract: Currently future nuclear reactor concepts of the Fourth Generation (Gen IV) are under development. ANTARES for example is the name of a Generation IV Very High Temperature Reactor (VHTR) concept (AREVA New Technology based on Advanced gas-cooled Reactors for Energy Supply). It is a helium cooled, graphite moderated modular reactor for electricity and hydrogen production, by providing the necessary process heat due to its high working temperature. To some extend the reactors need new, innovative materials developed just for this purpose.
Particular attention is given here to oxidation kinetics of new developed carbon materials like NBG-17 (Nuclear Block Graphite) with still unknown but needed information in context of severe air ingress accident in VHTRs. Special interest is paid to the Boudouard reaction, the oxidation of carbon by CO_2. In case of an air ingress accident, carbon dioxide is produced in the primary reaction of atmospheric oxygen with reflector graphite. From there CO_2 could flow into the reactor core causing further damage by conversion into CO. The purpose of current research is to ascertain if and to what degree this could happen.
First of all oxidation kinetic data of the Boudouard reaction with NBG-17 material is determined by experiments in a thermo gravimetric assembly. The measurements are evaluated and converted into a common formula and a Langmuir-Hinshelwood similar oxidation kinetic equation as input for VHTR reactor codes.

Objectives

The European RAPHAEL project (ReActor for Process heat, Hydrogen And ELectricity generation) is focused on the development of just one Generation IV reactor concepts, i.e. Very High Temperature Reactors (VHTR). This concept, which is called ANTARES (AREVA New Technology based on Advanced gas-cooled Reactors for Energy Supply) comprises a helium-cooled, graphite-moderated modular reactor for the production of electricity and hydrogen that provides the requisite process heat at extremely high temperatures. The primary focus of current research are the oxidation kinetics of the carbon-based materials (Nuclear Block Graphite) newly developed for this concept with respect to severe air ingress accidents in VHTRs, for which insufficient data is available as yet for a range of areas.

The components inside the cores of High Temperature Reactors are primarily made of graphite. This includes the matrix for the fuel, moderator and neutron reflector. These materials are optimised with respect to their behaviour under standard conditions. This includes their interaction with neutrons, their expansion properties and adequate long-term oxidative stability. Experimental tests with these materials have been performed in order to obtain data necessary for ensuring their safety in accidents involving graphite oxidation.

The graphite used in HTRs has a complex pore structure that affects the oxidation process. The oxidation kinetics of the HTR fuel element's graphites in oxygen–carbon reactions has already been investigated in a number of studies in the past. But the reaction equations empirically derived from these different investigations differ significantly from one another due to the relevant properties of the materials used in the tests. At present, the kinetic reaction data for these new materials, such as the specially developed NBG-17, are largely unknown. It is also, at present not possible to predict these materials' carbon dioxide-carbon reaction kinetics with any certainty, which therefore require further investigation. The oxygen tests conducted on these materials to date furthermore require complementation with tests involving the use of carbon dioxide as the oxidizing agent in order to gain a more complete understanding of the oxidation kinetics of graphite-based materials, and in order to be able to more accurately quantify the complexity of these kinetics under accident conditions.

The results of the oxidation kinetics experiments conducted on the structural graphite NBG-17 used in the ANTARES reactor under accident conditions in CO_2 (Boudouard reaction) will subsequently be discussed and used with the REACT/THERMIX simulation code to model selected HTR air ingress accident scenarios involving carbon dioxide-carbon reaction on the example of ANTARES.

Since oxidation may play an important role during heat treatment of graphite, e.g. when removing contaminants, the kinetics data generated by this study will also be relevant for later graphite treatment or even disposal and recycling.

Sample preparation

The objective of this experimental analysis is to determine the reaction kinetics of the new nuclear graphite NBG-17 produced by SGL. This concerns in

particular this material's Boudouard reaction kinetics at Regime II temperatures.

During a Boudouard reaction, solid graphite is oxidized to carbon monoxide as a result of oxidation by carbon dioxide and therefore converted from its solid into a gaseous phase. In this reaction, the graphite's change in weight by time is in direct proportion to the oxidation rate. Thermogravimetric analysers are designed to measure changes in weight by time in a defined atmosphere, at a defined temperature. The thermobalance system THERA2 was consequently built and set up to meet the requisite conditions.

The material to be analysed is the new nuclear graphite NBG-17 for which there are as yet no Boudouard reaction data available. This graphite is regarded as the optimum graphite for use in fuel blocks. It is similar to NBG-18, but was developed with a view to addressing the problem of gap formation between the composite material and blocks, i.e. it has a better thermal expansion coefficient.

The NBG-17 was derived from a semi-industrial batch, comprising two cuboids, and supplied in July 2007 by NRG Petten, Netherlands. The sample cuboids were respectively cut from the centre and edge of the industrially manufactured graphite block.

For comparison purposes, some of the experiments were repeated on the well-researched matrix material A3 and on NBG-17's sister graphite, NBG-18.

Since the thermobalance THERA2's measurement range is most accurate for samples weighing up to 250 mg, the samples prepared from the two NBG-17 cuboids therefore all weighed around 250 mg. In order to ensure that the peripheral conditions for the subsequent oxidation experiments would be as identical as possible, the size of the surface of the sample on the sample holder against which the gas would flow had to be kept as uniform as possible and the sample be right-angled. The size of the sample dish and the furnace pipe define a base area of no more than 10 mm x 10 mm.

Since metals, and transition metals in particular, have a catalytic effect during graphite corrosion, all contact with metal is strictly avoided during sample processing. Therefore the samples are cut using circular corundum and diamond saw blades that are clamped into a milling machine, which enables plane, uniformly thick (1.9 mm) slices to be cut from the cuboids with an accuracy of a tenth of a millimetre.

The samples' weight was subsequently adjusted as precisely as possible to 250 mg - by grinding the samples' narrow faces with corundum. The two reference values of weight and thickness thus give rise to largely uniform flow surfaces for all of the samples when placed into the thermobalance. Due to the non-angular shape of the original cuboid blocks, this approach was the easiest method to create these uniform flow surfaces.

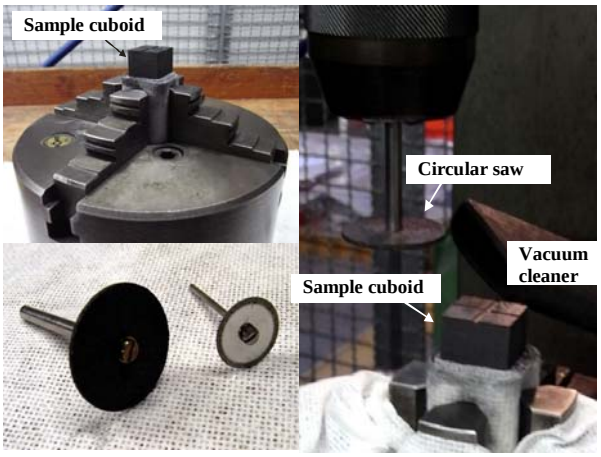

Figure 1: Tools used for sample preparation

After having been mechanically processed, all samples are cleaned for 15 minutes in an acetone ultrasound bath, turned, and cleaned again for another 15 minutes in the ultrasound bath. They are subsequently dried at 110°C for one hour inside a furnace.

Setting up the experiment

Before being able to start the actual measurements, the thermobalance, the interior of which is initially at atmospheric pressure, is calibrated to zero.

Once the sample has been successfully positioned inside the thermobalance, the balance is sealed and evacuated to 10^{-2} mbar by the vacuum pumps. Once fully evacuated, the system is filled with argon to 1250 mbar. If the required minimum pressure is not achieved, or if the system has not been used for a while, the evacuating and filling processes are repeated several times in order to clean it and check it for leaks. Since oxidation by CO_2 is more than ten times slower than oxidation by oxygen, any air inside the system would falsify the measuring results.

The system is brought to a pressure of 1000 mbar for the measurement. Once the valves leading into and out of the weighing chamber are closed, the sample chamber is purged with nitrogen, while the heavier argon remains in the lower-lying weighing chamber. In order to avoid disturbing the system's equilibrium and to ensure that, when switching to the oxidation gas, only the reaction kinetic effects rather than mechanical variations resulting from any changes in flow conditions are measured, the system is flushed at the same flow rate as used during the corrosion measurement.

The furnace is heated to the required target temperature at a heating rate of 10°C/min. The measured sample temperature can, in particular in the higher temperature ranges, be up to ~ 25°C lower than the set furnace temperature. This temperature variation also depends on

the furnace's insulation and ambient temperature. This is why, in order to achieve a certain sample temperature, the furnace's temperature usually has to be readjusted.

Once the pressure, temperature and flow rate have stabilised, the gas supply is switched to the oxidation gas. In earlier experiments with air, it was found that the selected flow rate of 150 ml/min provided the perfect balance between supplying an excess of oxidation gas and preventing the gas flow from disturbing the weighing balance. Since this flow rate ensures that there is an excess supply of the corrosion medium in the far more intensely progressing oxygen reaction, this flow rate will also ensure that there is an excess supply of the corrosion medium in the much more slowly-progressing Boudouard reaction.

The sample's current weight, as well as the date, time, pressure and temperature at each time step are recorded at 20-second intervals.

Once the required degree of oxidation has been achieved or the sample material has been fully consumed, the experiment is stopped and the gas supply is switched back to the purging gas (nitrogen). The furnace's temperature is then reduced to room temperature, first at 10°C/min, and once below 400°C, at a natural cooling rate, and subsequently switched off. If the graphite fully burns up, residues (ash) might be able to provide an insight into the material's purity.

In order to analyse the reaction kinetics of Regime II, it is necessary first to establish its temperature range. This is achieved with the aid of a transient test, during which the graphite's oxidation rate is determined by measuring its weight loss by time at a gradually increasing temperature. The other variables applied for covering the temperature range of 1150 - 1450°C during this test included a continuous gas flow rate of 150 ml/min of 20% CO_2 in N_2 and a heating rate of 3°C/min.

For analysis, the logarithm of the reaction rate was plotted against the inverse of the temperature in °C in an Arrhenius plot (Figure 2). Although this method does not adequately take into account the effect of burn-off, the graph does give a clear indication of the reaction regimes.

This data shows that the temperature range of relevance to this investigation and of Regime II is 1175°C to 1275°C. Since the transient test involves the use of a temperature ramp and the reaction rate is measured by loss of weight, the rate of the associated temperature lags slightly behind. This gives rise to a comparatively fuzzy-definition of the regime's boundaries to lower temperatures. It was consequently necessary to find a compromise between using a low heating rate for generating more clearly-defined boundaries and a heating rate that is sufficiently high to ensure adequate material availability even at high temperatures despite progressive corrosion. The temperature range under investigation was thus increased to 1150°C to 1275°C.

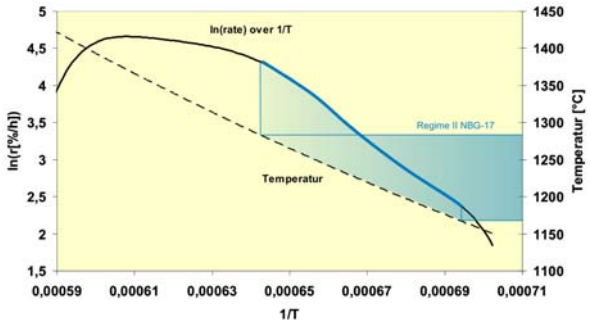

Figure 2: Logarithm of the reaction rate of NBG-17 at 20% CO_2 in N_2 over 1/T relative to the temperature used to determine Regime II

Table 1 lists the number of tests conducted within a temperature range of 1150°C to 1275°C at different CO_2 concentrations, divided into regime core range (1175-1250°C) and regime boundary range (1150°C and 1275°C). These tests furthermore included one blank test respectively in order to compensate for flow- and temperature effects, and transient tests. The letters E and C indicate the location within the graphite cuboids from which the samples used in the tests were prepared. E (edge) stands for the cuboid taken from the graphite block's edge and C (centre) for the cuboid taken from the centre of the industrially manufactured raw graphite block.

Table 1: Test matrix of tests conducted on NBG-17 centre (C) and edge (E)

Temperature [°C]	1150		1175		1200		1225		1250		1275	
	C	**E**	**C**	**E**	**C**	**E**	**C**	**E**	**C**	**E**	**C**	**E**
10% CO_2 in N_2	3	3	3	3	5	3	3	3	3	3	3	3
20% CO_2 in N_2			3	3	3	3	3	3	5	5	3	3
100% CO_2	3	3	3	3	3	4	3	3	3	4		

The first results on the reaction kinetics of the nuclear graphite NBG-17 were compared with the well-known matrix material A3-3, which is a subgroup of the matrix material A3. A range of spot tests on NBG-17's sister graphite, NBG-18, were also performed for comparison purposes.

Results

The NBG-17 samples obtained from the centre respectively the edge of the block exhibit some very strong differences with respect to their reaction rates when tested under the same conditions.

The materials where consequently submitted for other material analyses in order to investigate other factors that can affect reaction rates, such as porosity and

impurities. As the two samples' reaction rates approximated one another in most cases after approximately 50% burn-off, it is unlikely that the observed differences are caused by the catalysis of impurities, the mass spectrometry measurements show no significant differences between them.

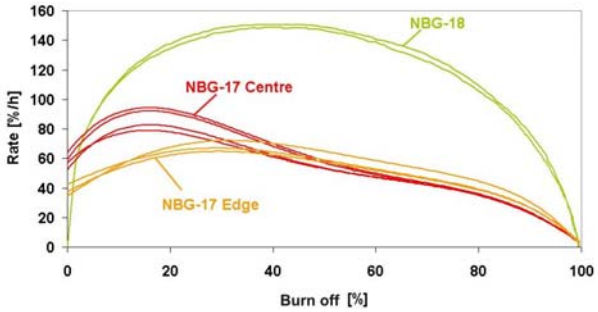

Figure 3: Reaction rate of NBG-17 (centre and edge) an NBG-18 at 1200°C in 100% CO_2 over burned off material

The most likely explanation for this difference is that the samples' pore structures differ. These differences could be due to the graphite block not having been evenly impregnated during manufacture, or of the binder in the graphite's block interior not having been as fully graphitised as the binder on its outside. Since the sample material was obtained from a semi-industrial batch, it is possible that it suffered from certain imperfections that would be absent in a technically perfected sample. Due to the small size of the cuboids of material obtained, it is unfortunately also not certain whether the differences in the material are a general problem concerning the material's density across this graphite block's entire cross section, or whether this is a localised phenomenon.

A comparison of the NBG-17 graphite with its 'sister' graphite NBG-18 showed that the two graphites' reaction rates are extremely different. As far as is known, both of these materials are manufactured from the same raw materials using the same process. Their main difference is only their maximum grain size. However, the reason for the near two-fold increase in reactivity is not finally proved.

The three reaction regimes of the Boudouard reaction for NBG-17 were successfully determined and the data necessary for determining the reaction kinetics of Regime II in steps of 25°C for three different concentrations were successfully collected.

The materials obtained for the study from the centre and the edge of the manufactured block exhibited different reaction behaviours. This difference may the due to the semi-industrial production of this batch. It is not, however, known whether the differences within the material comprise a general phenomenon that affects the material across its entire cross section, or a random, localised occurrence.

The Boudouard reaction of NBG-17 takes place in Regime II at temperatures between 1150°C to 1275°C. This is in agreement with the simplified kinetic equation:

$$RG' = 2308{,}9 \cdot \exp\left(-\frac{24300}{T}\right) \cdot \sqrt{p_{CO_2}} \cdot \qquad (1)$$

In this temperature range, the NBG-17 graphite's apparent activation energy for corrosion by carbon dioxide is

$$E_A' = 202 \pm 1\% \ \frac{kJ}{mol} \qquad (2)$$

The reaction kinetics can be expressed using a Langmuir-Hinshelwood-like formula

$$RG = -\frac{625 \cdot \exp\left(-\frac{5000}{T}\right) \cdot p_{CO_2}}{1 - 0{,}231 \cdot \exp\left(\frac{30000}{T}\right) \cdot \sqrt{p_{CO_2}}} \left[\frac{mol_C}{m^2 s}\right] \qquad (3)$$

The thermogravimetric analyser THERA2 reaction rate measurements of the carbon dioxide oxidation of NBG-17 have a measuring accuracy of 11.26% and a relative probable error of 8%. The differences between the NBG-17 samples taken from the centre and edge of the industrially manufactured NBG-17 graphite block consequently have a heavier weighting than the measuring errors.

Since basic data are essential to an understanding of corrosion behaviour in accident events, the data on the Boudouard reaction's reaction kinetics collected as part of this study should be further validated. However, the present experimental results are totally and fully adequate for an initial assessment of air ingress accident scenarios, although safety-related predictions that require precision should never be made on the basis of one source and set of data alone, as a single test does not equal 'testing'.

Outlook

The data of this study can be validated by repeating the series of experiments conducted on NBG-17 using material from another batch of NBG-17. It would furthermore be advisable to compare the measured data obtained with the THERA analyser with measuring data obtained with other equipment. Expansion of the experimental conditions to include other partial carbon dioxide pressures would increase the accuracy of the range of less than 21% that is of interest for the simulation. The kinetic data of the new NBG-17 graphite could furthermore be made more

comprehensive by conducting corrosion experiments with oxygen and water vapour (humidity) experiments. The effect of the reaction product CO on the reaction rate also requires further investigation.

Further investigations are also required in order to make the information on the corroded samples' porosity and strength more comprehensive. This would also make it easier to assess the bottom reflector's structural-mechanical thresholds and the consequences of exceeding these thresholds.

It is furthermore important to ensure that the graphite oxidation reaction rates modelled in these experiments accurately reflect real-scale oxidation behaviour by conducting larger scale tests.

It is also advisable to use the new kinetic data to model other delayed air ingress scenarios, as have been performed in [1, 2] using old data.

The effect of geometry changes as a result of graphite corrosion in air ingress accidents is also very important, and the development of suitable calculational tools, supported by experimental data, will be vital in order to fully do this effect justice.

Accident scenarios and their boundary conditions might also benefit from a review. On the one hand, this is with respect to both basic safety and the probability of their occurrence, and on the other hand, also with respect to their presumed consequences and the sequence of the processes involved. A spontaneous drop in pressure of 70 bar has the potential of creating a great range of active forces and could potentially cause geometric changes in the reactor vessel's interior and position, or state.

The kinetic data for the Boudouard reaction can also be applied with respect to the disposal of irradiated graphite by removing the ^{14}C from the material by oxidation. The radiocarbon is generated primarily from nitrogen and therefore rarely forms part of the graphite's lattice, but is bound mainly to the areas near the surface and inner pores. This is why the activation energy of ^{14}C within the graphite lattice is noticeably lower than that of ^{12}C. The aim here is to remove the active ^{14}C from the graphite by oxidation without causing any damage to the graphite itself. This is why the activation energy of the graphite reaction should be as high as possible while still allowing the ^{14}C in the graphite near its surface to be oxidised. To date, this has been achieved successfully using 1% oxygen in nitrogen and with water vapour. Due to the reaction kinetics of the Boudouard reaction, which are similar to that of water vapour oxidation, the concept of removing the ^{14}C from graphite through the use CO_2 holds great promise and requires further investigation. [3].

References

[1] Haque, H., Brinkmann, G., 2006. Consequences of delayed air ingress following a depressurization accident in a high temperature reactor, Proc. HTR2006 3rd Int. Top. Mtg. on High Temperature Reactor Technology, October 1-4, 2006, Johannesburg, South Africa

[2] Haque, H., Brinkmann, G., Feltes, W., 2004. Thermal response of a modular high temperature reactor during passive cooldown under pressurized and depressurized conditions, Nuclear Engineering and Design 236 (2006) 475–484

[3] Florjan, M., 2009. Dekontamination von Nukleargraphit durch thermische Behandlung, PhD thesis, RWTH Aachen

Simulating the Cold He Gas Ingress Transient of the OECD-NEA Benchmark "PBMR Coupled Neutronics/Thermal Hydraulics Transient Benchmark The PBMR-400 Core Design"

C. Druska, K. Nünighoff, Ch. Pohl

Institute for Energy Research - Safety Research and Reactor Technology (IEF-6), Forschungszentrum Jülich
Corresponding author: k.nünighoff@fz-juelich.de

Abstract: Simulations of the OECD-NEA benchmark "PBMR Coupled Neutronics/Thermal Hydraulics Transient Benchmark – The PBMR-400 Core Design" were performed with TINTE and MGT. In this transient a bypass valves opens and cold helium gas flow into the gas inlet plenum. The change of the gas inlet temperature will effect the neutronic behavior via thermal hydraulic feedback. A code-to-code comparison between TINTE and MGT results will be presented. The influence of a new developed cross section library on the transient behavior of the reactor will be investigated. Later, a comparison with internationally applied coupled neutronic/thermal hydraulic codes will be envisaged.

Introduction

Aim of the OECD-NEA benchmark "PBMR Coupled Neutronics/Thermal Hydraulics Transient Benchmark – The PBMR-400 Core Design" [1] is to establish well defined problems, based on a common set of cross sections, to compare methods and tools in core simulation and thermal-hydraulics analysis with a specific focus on transient events through a set of multi-dimensional computational test problems. By calculating this benchmark the results of the Juelich reactor codes TINTE [2] and its multi-group derivate MGT will face up to an international code-to-code comparison. A second motivation for calculating this benchmark is its possibility to intensively test the new developed TISPEC cross section library for TINTE/MGT based on the latest evaluated ENDF data [3].

This transient simulates an incident where a malfunction of a bypass valve occurs. This causes cold helium gas to flow into the upper gas inlet plenum and reducing the gas inlet temperature by 10 % of its nominal value of T=500 K during the next 10 s. After a period of 300 s it is assumed that the reactor safety system closes the valve again. After closing the bypass valve the inlet temperature increase during 10 s to the nominal value again. During the transient no control rod positons, mass flow, and pressure will be kept constant.

Behaviour of a reactor after cold helium ingress

One consequence of the reduction of the gas inlet temperature from T=500 K to T=450 K is the Doppler feedback on the resonance absorber cross section ^{238}U. The reduced gas temperature reduces the surface temperature and later also the fuel temperature. Fig. 1 shows the averaged fuel temperature as function of time. It can be seen, that the averaged fuel temperature is lowered by $\Delta T \approx 4$ K during the first 40 s. Then the temperature increases and after t=340 s decreases and a new —approximately $\Delta T = 2$ K higher than the starting temperature— level is reached.

All three simulations agree within a few Kelvin, i.e. a maximum deviation between MGT with the new cross section library and TINTE of less than 0.4 % is observed.

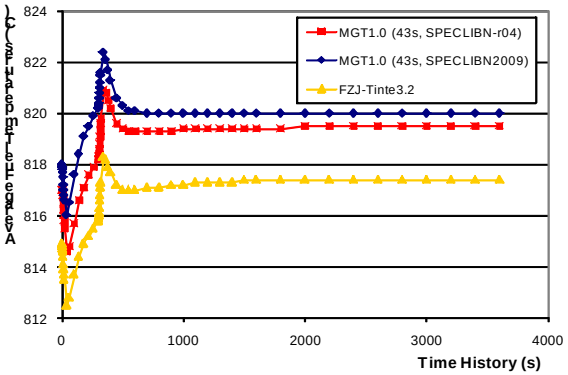

Fig. 1 Fuel temperature averaged over the whole core as function of time for a TINTE and two MGT simulations. The MGT calculations were performed with the old library (SPECLIBN-r04) and the new ENDF-B-VII based library (SPECLIBN2009).

A different observation could be made when looking for the maximum fuel temperature in the core as function of time shown in Fig. 2. In contrast to the average fuel temperature, the maximum fuel temperature immediately starts to increase. After t=300 s the maximum fuel temperature decreases again. However, the new temperature level is slightly higher than the starting temperature. However, both codes agree within 2 %. The new library influence the maximum fuel temperature in the way, that less than 0.5 % lower temperatures are calculated.

This contradictive observation can be explained when analyzing the axial temperature profiles at certain radial positions for two different time points. Fig. 3 illustrates the fuel temperature for three radial positions at t=0 s and t=40 s.

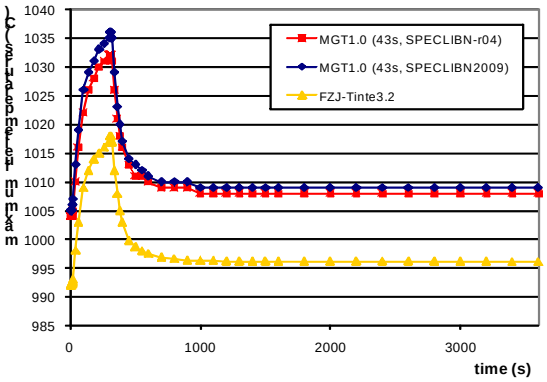

Fig. 2 Maximum fuel temperature as function of time for a TINTE and two MGT simulations. The MGT calculations were performed with the old library (SPECLIBN-r04) and the new ENDF-B-VII based library (SPECLIBN2009).

It can be seen, that at the top of the core the temperature is reduced by approximately 20 K during the first 40 s. At a distance of 2 m from the top of the core the fuel temperature shows no significant deviations. Further, approximately 8 m inside the core the fuel temperature shows a maximum. It can be seen, that after 40 s the maximum temperature is increased.

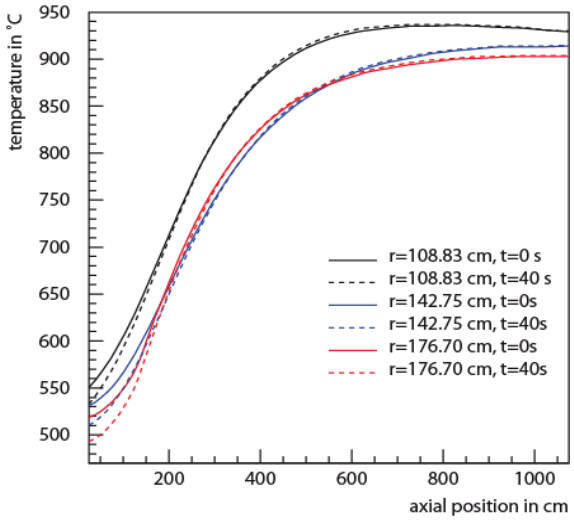

Fig. 3 Axial temperature profile of the fuel temperature for two different time points and three radial positions.

The lowered fuel temperature at the top of the reactor core causes a narrowing of the resonances of the (n,γ) absorption cross section and thus the absorption rate of thermal neutrons is reduced. This leads to an increase of reactivity and an increase of the reactor power as shown in Fig. 4. An total increase of 14 % is observed. The deviation between all three simulations is lower than 0.5 %.

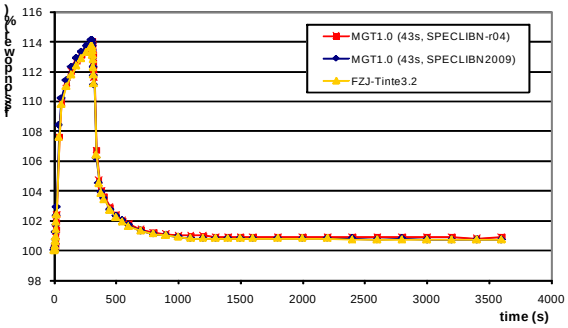

Fig. 4 Relative fission power as function of time for a TINTE and two MGT simulations. The MGT calculations were performed with the old library (SPECLIBN-r04) and the new ENDF-B-VII based library (SPECLIBN2009).

Conclusion and Outlook

A reactivity transient caused by a cold He gas ingress due to a malfunction bypass valve was investigated. The behavior of the reactor during such an incident was analyzed and could be explained.

Both codes as well as old and new nuclear data library agree on a sub percent level.

After the results of the benchmark will be published MGT will be confronted with the results of various computer codes available for transient analysis with coupled neutronic/thermal hydraulic codes for pebble bed high temperature gas cooled reactors world wide.

References

[1] http://www.nea.fr/html/science/wprs/pbmr400/

[2] H. Gerwin, *Das zweidimensionale Reaktordynamikprogramm TINTE - Teil 1: Grundlagen und Lösungsverfahren*, Jül Bericht 2167, KFA Jülich (1987).

[3] Nuclear Data Sheets 107(2006)12

Simulating the Steady State Cases of the OECD-NEA Benchmark "PBMR Coupled Neutronics/Thermal Hydraulics Transient Benchmark The PBMR-400 Core Design"

C. Druska, K. Nünighoff, Ch. Pohl

Institute for Energy Research - Safety Research and Reactor Technology (IEF-6), Forschungszentrum Jülich
Corresponding author: c.druska@fz-juelich.de

Abstract: Simulations of the OECD-NEA benchmark "PBMR Coupled Neutronics/Thermal Hydraulics Transient Benchmark – The PBMR-400 Core Design" were performed with TINTE and MGT. Here, results of different steady state scenarios will be presented. A pure thermal hydraulics scenarios with given heat sources as well as a coupled neutronics / thermal hydraulic scenario with given nuclide densities in the core regions was simulated. The temperature coefficients and control rod worth were analyzed in two different scenarios with TINTE and MGT. Later, the results will allow for an international comparison of different reactor dynamic codes applied for transient analysis of high temperature gas cooled reactors.

Introduction

Aim of the OECD-NEA benchmark "PBMR Coupled Neutronics/Thermal Hydraulics Transient Benchmark – The PBMR-400 Core Design" [1] is to establish well defined problems, based on a common set of cross sections, to compare methods and tools in core simulation and thermal-hydraulics analysis with a specific focus on transient events through a set of multi-dimensional computational test problems. By calculating this benchmark the results of the Juelich reactor codes TINTE [2] and its multi-group derivate MGT will face up to an international code-to-code comparison. A second motivation for calculating this benchmark is its possibility to intensively test the new developed TISPEC cross section library for TINTE/MGT based on the latest evaluated ENDF data [3]. This article focuses on the steady state scenarios of the above mentioned benchmark:

- Thermal hydraulic solution with given power/heat sources
- Combined neutronic/thermal hydraulic calculation (starting condition for transients)
- Determination of Doppler, moderator, and reflector temperature coefficient
- Determination of control rod worth for control rods removed

Thermal hydraulic solution with given heat sources

In this scenario only the thermal hydraulic part of the code system should be applied. The heat sources were provided and included in the reactor model as external heat sources in the 110 core regions. Thus the fuel and moderator temperature can only be calculated in TINTE and MGT while the neutronic part is running a pseudo coupled neutronic thermal hydraulic simulation was performed. Here, the fission power was set to 1 MW, i.e. less than 1 % from the nominal power of 400 MW given by the external heat sources, and the influence of the neutronic part of the simulation can be assumed negligible. Simulations have been performed with TINTE (2-group-polynomial cross section representation), a 2-group-polynomial MGT calculation, and a full 43 multi-group simulation with internal spectrum calculation.

The axial power profile averaged over all five radial core zones is plotted in Fig. 1. It can be seen, that a very nice agreement of all codes and cross sections representations could be achieved.

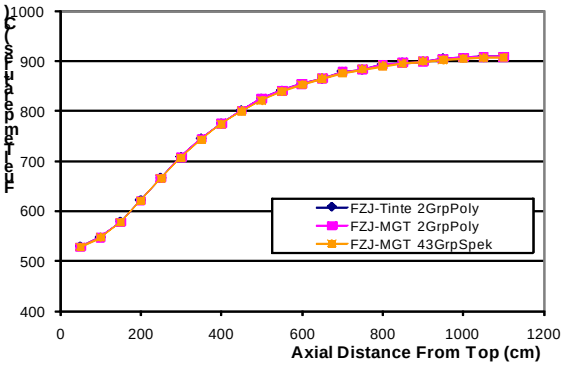

Fig. 1 Axial fuel temperature profile averaged over all radial core zones calculated with TINTE and MGT.

As the thermal hydraulic part in MGT is the same as in TINTE this result was expected and proves, that no serious errors have been inserted during the development of MGT.

Combined neutronic/thermal hydraulic calculation

In the next step a coupled neutronic/thermal hydraulic simulation of the core with given nuclide densities in the 110 core zone was performed. As the mid column of the reactor model is not cooled all the energy should be deposited local, i.e. all released energy is deposited in the core. This was realized in TINTE and MGT with the option LPOW. Without this assumption an overheating of the central reflector would occur and would strongly influence the coupled thermal hydraulic calculation.

This is the simplest scenario to be simulated with TINTE or MGT, but serves as the starting condition for all later transient cases. This means, a wrong description of this steady state scenario would drastically influence the transient results.

Fig. 2 shows the axial power profile averaged over all five radial core zones. The steady state was simulated with TINTE. Then the influence of the multi group approach was stepwise investigated. First, a 2-group calculation with polynomial cross section representation –equivalent to a TINTE calculation- was performed. As can be seen in Fig. 2 both simulations agree very well.

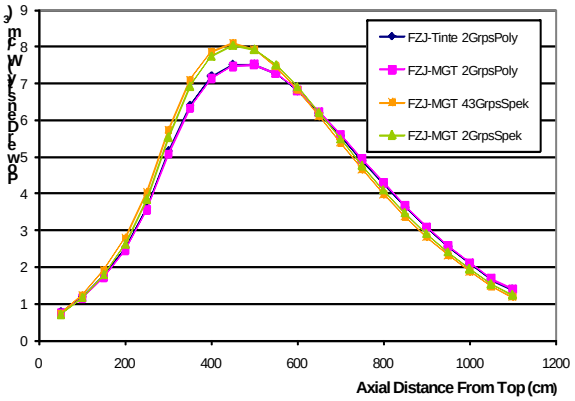

Fig. 2 Axial power profile averaged over all radial core zones for different MGT simulations compared with TINTE.

The second MGT simulation was a calculation with tow energy groups too, but with internal spectrum calculation. As slight shit up to the top reflector of the power profile could be observed. In the last step the number of neutron energy groups was expanded from two to full 43 groups. Here, only minor changes were observed. It could be concluded, that the internal spectrum calculation –which is assumed to be more precisely- causes the main differences between TINTE and MGT.

This steady state was further used to investigate the influence of the old TISPEC library and the new TISPEC library based on ENDF-B-VII data. Fig. 3 shows the axial profiles averaged over the radial core zones for the power, fast neutron flux, and thermal neutron flux. No significant change of the results could be observed. The power density profiles show no serious deviations between old and new library. The mean deviation is 0.23 %. The maximum deviation is 2.26 % and is located in the lower most 50 cm of the core. Furthermore, it can be noticed that position of the maximum of the axial power profile as well as that of the neutron fluxes is –within the spatial resolution of mesh– at the same position and not influenced by the new library.

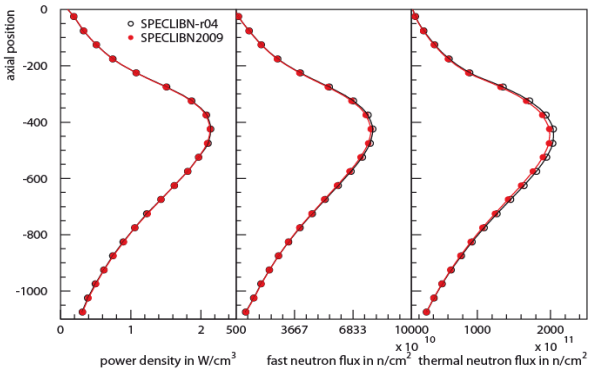

Fig. 3 Comparison of averaged axial profiles between SPECLIBN-r04 and ENDF-B-VII based SPECLIBN2009: radial averaged axial power profile (left), radial averaged fast neutron flux profile (center), and radial averaged thermal neutron flux profile (right).

Outlook

After the results of the benchmark will be published MGT will be confronted with the results of various computer codes available for transient analysis with coupled neutronic/thermal hydraulic codes for pebble bed high temperature gas cooled reactors world wide.

References

[1] http://www.nea.fr/html/science/wprs/pbmr400/
[2] H. Gerwin, *Das zweidimensionale Reaktordynamikprogramm TINTE - Teil 1: Grundlagen und Lösungsverfahren*, Jül Bericht 2167, KFA Jülich (1987).
[3] Nuclear Data Sheets 107(2006)12

Infinite Diluted Cross Sections for TINTE/MGT Based on ENDF-B-VII

K. Nünighoff, C. Druska

Institute for Energy Research - Safety Research and Reactor Technology (IEF-6),
Forschungszentrum Jülich
Corresponding author: k.nünighoff@fz-juelich.de

The nuclear data base of TINTE and its successor MGT is based on the 43 group MUPO library of the Dragon project. A decision was made to update the library to the international evaluated ENDF-B-VII data. The ENDF-B-VII raw data were processed with NJOY and converted to the MUPO based TISPEC cross section library usable for TINTE/MGT. As the nuclear cross sections of the Juelich core design code V.S.O.P. have been updated to ENDF-B-VII too, now both Juelich reactor codes are now using the same nuclear data basis.

Introduction

The spectrum code for infinite lattice calculations in TINTE [1] and MGT called TISPEC is based on the MUPO code[2] and its 43 group cross section library [3,4] developed in the 1960's years. This article will describe the update of the infinite diluted cross sections to international evaluated ENDF-B-VII data [5]. The TISPEC library was extended by 21 nuclides and now comprises 224 nuclides. All cross sections were processed for a typical temperature inside a high temperature gas cooled reactor of T=900 K –i.e. the same temperature the nuclear cross sections of V.S.O.P. [6] were made for.

Generation of 43 Groups Cross Section Library

The structure of the cross section data sets differs between fissile and non fissile materials. For non-fissile materials only the transport cross section σ_{trans} and the absorption cross section $\sigma_{abs.}$ were provided on the library tape. The transport cross section σ_{trans} is defined as:

$$\sigma_{trans} = \sigma_{(n,\gamma)} + \sigma_{fiss.} + \sigma_{inelas} + \sigma_{elas.}(1 - \frac{2}{3 \cdot A})$$

Here, A is the mass number of the isotope. The absorption cross section is the sum over all neutron nucleus interactions absorbing the incident neutron:

$$\sigma_{abs.} = \sigma_{(n,\gamma)} + \sigma_{inelas.} + \sigma_{fiss.}$$

The data sets of fissile materials contain two additional cross section sets: the fission cross section $\sigma_{fiss.}$ and the fission cross section weighted with the energy dependent mean number of emitted neutrons $\nu\sigma_{fiss.}$.
The ENDF-B-VII raw data were processed with the NJOY code system [7] by applying the following modules in the listed order.

1. reconr → reconstruction of resonances and generation of point wise cross sections
2. broadr → Doppler broadening of the point wise cross section to adjust the desired temperature of T=900 K
3. groupr → generation of multi group cross sections

Within the module groupr the point wise cross section were condensed to the multi group cross sections according to the well known equation given below.

$$\sigma_G = \frac{\int_{E_{low}}^{E_{high}} F(E)\sigma(E)\phi(E)dE}{\int_{E_{low}}^{E_{high}} \phi(E)dE}$$

For some nuclides like ^{10}B or ^{6}Li additional nuclear reaction cross sections were taken into account to correctly determine the absorption cross section. As an example for a non fissile material the cross section of ^{10}B is shown in Fig. 1. Here, the new cross section based on ENDF-B-VII data is compared with the old MUPO based cross sections. For completeness the ENDF-B-VII point data are also shown.

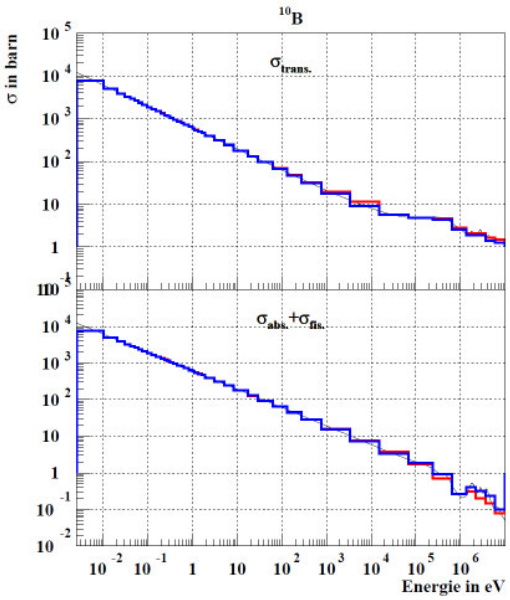

Fig. 1 Transport cross section and absorption cross section based on ENDF-B-VII (blue line), MUPO (red line), and ENDF-B-VII point data (black curve) for ^{10}B.

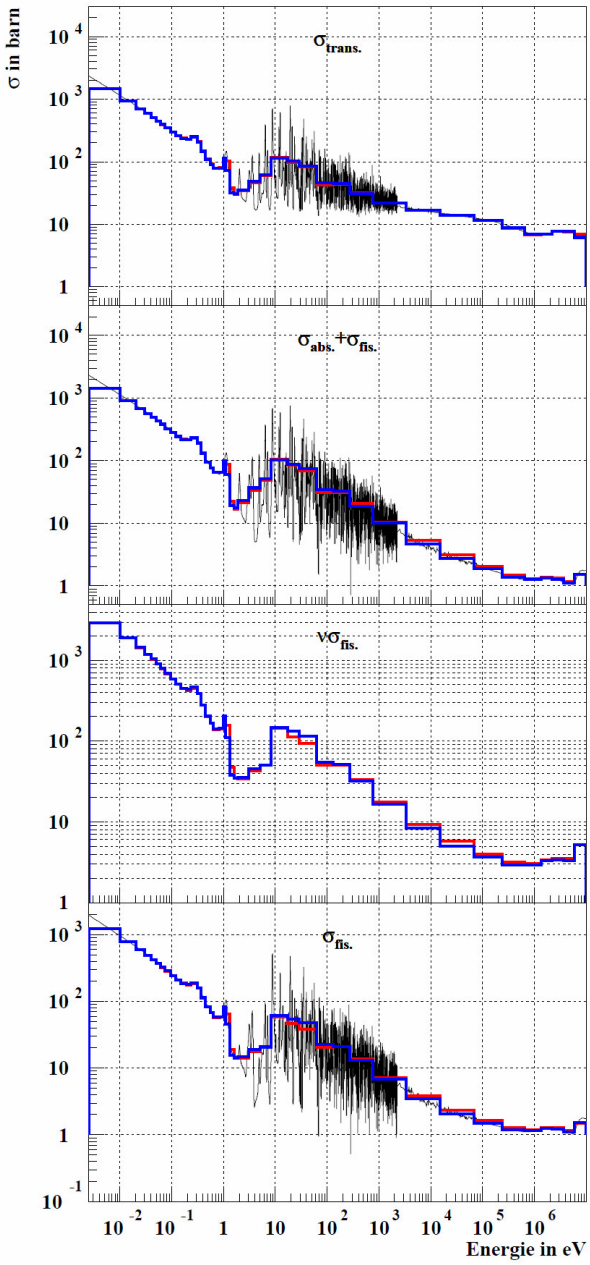

Fig. 2 Transport cross section $\sigma_{trans.}$, absorption cross section $\sigma_{abs.}$, $\nu\sigma_{fiss.}$, and fission cross section $\sigma_{fiss.}$ based on ENDF-B-VII (blue line), MUPO (red line), and ENDF-B-VII point data (black curve) for the fissile nuclide ^{235}U.

Fig. 2 shows the cross section data set for the fissile material ^{235}U. The additional data for $\nu\sigma_{fiss.}$ and $\sigma_{fiss.}$ are plotted. Here, the new processed group cross sections based on ENDF-B-VII (blue line) are compared with the old TISPEC data (red line) and the ENDF-B-VII point data (black curve).

In order to study the influence of the new library on simulations performed with MGT, steady state conditions of a PBMR 400 like reactor were simulated. The influence of each single isotope on k_{eff} was determined by replacing the appropriate nuclide in the old library with the new processed data set. The difference of Δk_{eff} between the old MUPO based library and the new ENDF-B-VII data based library is shown in Fig. 3 for the transuranic elements and graphite and in Fig. 4 for the fission products. The largest effect of Δk_{eff}=663 mNile is due to ^{235}U. Simulating the same with the old and new library shows an reactivity increase of Δk_{eff}=1.18 Nile.

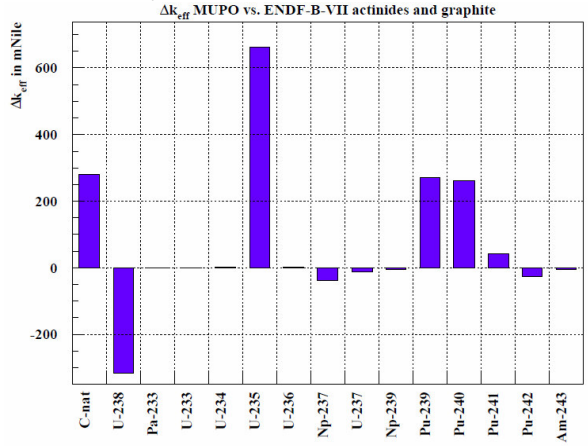

Fig. 3 Difference in k_{eff} for various transuranic elements and graphite when replacing the old MUPO based library with new data sets based on ENDF-B-VII.

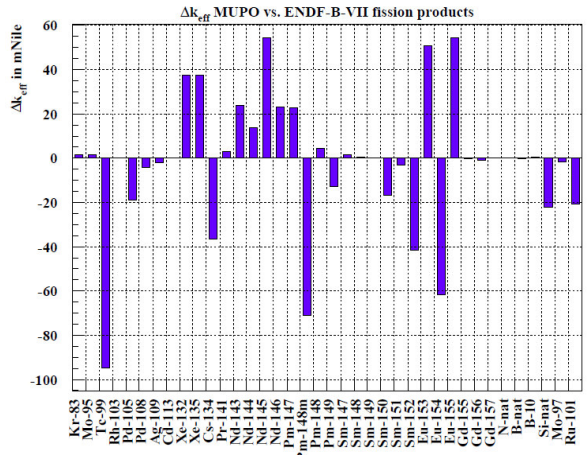

Fig. 4 Difference in k_{eff} for various fission products when replacing the old MUPO based library with new data sets based on ENDF-B-VII.

New Graphite Data

The new developed graphite absorption cross section differs from the old MUPO based library SPECLIBN-r04 as can be seen in Fig. 5. This differences are due to the fact, that the old library assumes a certain amount of impurities in the graphite and thus the thermal absorption cross section $\sigma_{abs.}$(2200 m/s) is higher. Whereas the ENDF-B-VII data specifies a thermal absorption cross section of $\sigma_{abs.}$(2200 m/s)=3.367 mbarn the old library SPECLIBN-r04 is based on a thermal absorption cross section of $\sigma_{abs.}$(2200 m/s)=3.73 mbarn. A first calculation with the new library delivers a 1.016 Nile higher value for k_{eff} due to the reduced absorption rate

of neutrons in graphite. For a next calculation the absorption cross section was renormalized according to the assumed value hard wired in the TINTE and MGT code:

$$\sigma_{abs.}^{renorm.} = \sigma_{abs.}^{ENDF-B-VII} \cdot \frac{3.73\ mbarn}{3.367\ mbarn}$$

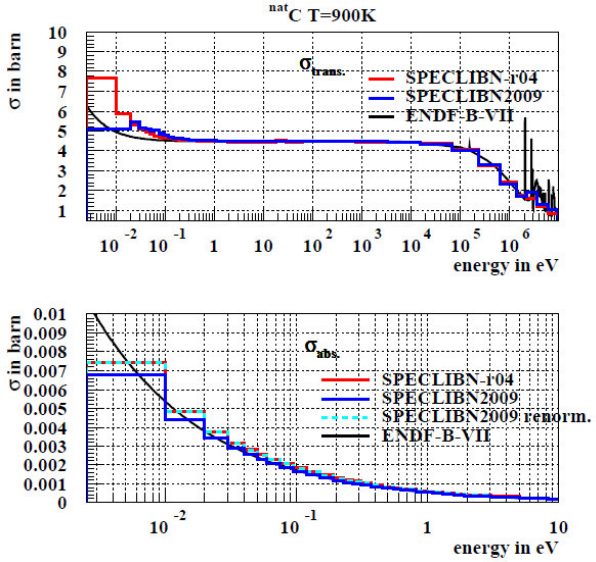

Fig. 5 Transport and absorption cross section for graphite (^{nat}C). A comparison between old library (SPECLIBN-r04) and new library (SPECLIBN2009) is shown.

Due to the increased absorption cross section the absorption rate of neutrons in the graphite was increased too resulting in a lower value for k_{eff}. For the renormalized cross section set the new library results only in a 298 mNile higher value for k_{eff}. The absorption cross section for graphite below 10 eV is shown in the lower panel of Fig. 5. The better agreement of the renormalized cross section with the old nuclear data library can be seen. To proof the correctness of the new cross sections experimental data of the total cross section measured by Bowman et al. [8] in the thermal energy range and Danon et al. [9] for the keV range are confronted with the new ENDF-B-VII based total cross section as shown in Fig. 6. The thermal energy range as well as the fast energy range is in a very good agreement with experimental data. The peaks in the thermal experimental data are due to neutrons scattered at different layers of the graphite crystal.

Conclusion and Outlook

The new nuclear data library SPECLIBN2009 providing the cross sections for the spectral code TISPEC in TINTE/MGT was updated to ENDF-B-VII. The hard wired absorption cross section for graphite in MGT will be replaced by a variable provided in the tn4-file in a manner, that the old library using the hard wired cross section can be used too.

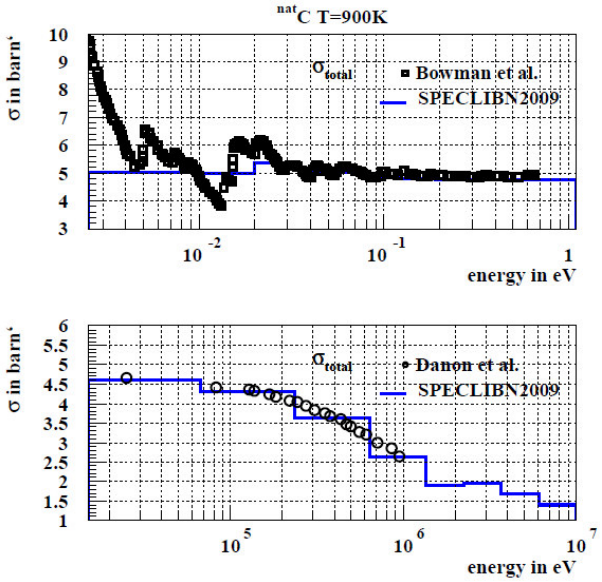

Fig. 6 Total cross section of graphite from newly generated graphite cross sections based on ENDF-B-VII compared with recently measured data by Bowman et al. [8] and Danon et al. [9].

References

[1] H. Gerwin, *Das zweidimensionale Reaktordynamikprogramm TINTE - Teil 1: Grundlagen und Lösungsverfahren*, Jül Bericht 2167, KFA Jülich (1987).

[2] J. Schlösser , *MUPO AN IBM-7090 PROGRAMME TO CALCULATE NEUTRON SPECTRA AND MULTI-GROUP CONSTANTS*, Dragon Project Report 172 (1963).

[3] U. Nyffenegger and J. Schlösser, *The New Cross Section Library of the Dragon Project*, Dragon Project Report 261 (1964).

[4] L. Massimo, *The MUPO Nuclear Data Library 5*, Dragon Project Report 814 (1972).

[5] Nuclear Data Sheets 107(2006)12

[6] H.J. Rütten et al, *V.S.O.P.(99/05) Computer Code System*, Jül-4189, Forschungszentrum Jülich (2005).

[7] R.E. MacFarlane and D.W. Muir, *The NJOY Nuclear Data Processing System, Version 91*, LA-12740-M, Los Alamos National Laboratory (1994).

[8] C.D. Bowman et al., *Measurements of Thermal Neutron Diffraction and Inelastic Scattering in Reactor-Grade Graphite*, Nucl.Sci.Eng. 159(2008)182-198

[9] Y. Danon et al., *Beryllium and Graphite High-Accuracy Total Cross-Section Measurements in the Energy Range from 24 to 900 keV*, Nucl.Sci.Eng. 161(2009)321-330

Kopplung des Monte-Carlo-Codes MCNP und des Aktivierungscodes FISPACT mit automatischer Visualisierung der Simulationsergebnisse

P. Bourauel, R. Nabbi

FZ Jülich, Institut für Energieforschung, Leo-Brandt-Strasse, D-52428 Jülich
Corresponding author: p.bourauel@fz-juelich.de

Einleitung

Der 3D Monte-Carlo Computercode MCNP [1] wird neben Kritikalitätsberechnungen für kerntechnische Systeme auch für die Simulation des Strahlen- und Partikeltransports benutzt. Die daraus gewonnenen Ergebnisse über die Neutronenflussverteilung und der dazugehörigen Spektra erlauben es, mit Aktivierungscodes wie FISPACT [2] und den entsprechenden nuklearen Datenbanken Aussagen über die Materialaktivierung, nukleare Aufheizung und Strahlenschäden zu erlangen.
Durch den stochastischen Charakter der Teilchen- und Strahlentransportvorgänge werden die Ergebnisse mit den Materialzellen verknüpft, aus denen das Geometriemodell von MCNP aufgebaut wird. Ist eine hohe räumliche Auflösung für die Flux-Mapping- und Aktivierungsberechnungen mit FISPACT erforderlich, wird eine feine Segmentierung der MCNP-Geometrie zwingend, was wiederum einen beträchtlichen Aufwand für den Modellierungsprozess bedeutet. Aus diesem Grunde werden weltweit mehrere Simulationsmethoden entwickelt mit dem Ziel, die Datenübergabe zwischen MCNP und FISPACT zu automatisieren und zu optimieren [3].

In der vorliegenden Arbeit wird eine neue Methode vorgestellt, welche eine geometrische Segmentierung für einen gekoppelten Einsatz von MCNP und FISPACT vornimmt, indem sogenannte, überlagerte Mesh-Tallies und interne Partikelverfolgung (Particle Tracing) kombiniert werden. Das Verfahren bietet ebenfalls eine Routine zur detaillierten graphischen Darstellung bzw. Visualisierung der Aktivierungs-analyse, sowie der Neutronenflussverteilung über die gesamte Geometrie eines jeden beliebigen Modells. Die Methode wurde aus dem Bedarf hinaus entwickelt, das Modell mit dem Aufbau eines Port Plugs, als Komponente für den internationalen Fusionsreaktor ITER, neutronenphysikalisch zu untersuchen. Durch die komplexe Geometrie des Bauteils und fortlaufenden Änderungen innerhalb des Designprozesses soll das neue Verfahren eine effiziente und zeitsparende Analyse für jede mögliche Konfiguration erlauben.

Beschreibung des ITER Port Plugs

Einer der komplexen Port Plugs beinhaltet das sogenannte Ladungsaustausch-Rekombinations-spektrometer (CXRS), das der Erfassung und Analyse der elektromagnetischen Strahlung aus dem Plasmabereich und den Randschichten der Fusionskammer dient. Das System wird in einem der oberen Port Plugs installiert und besteht aus zahlreichen Komponenten, wie Glasfaseroptische Kanäle, Spektrometer und Detektoren (Abb. 1).

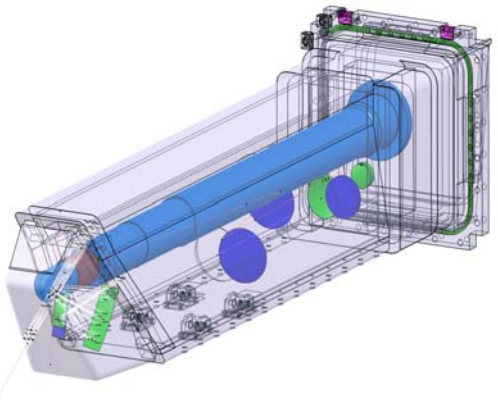

Abb. 1: Detailmodell des Port Plug

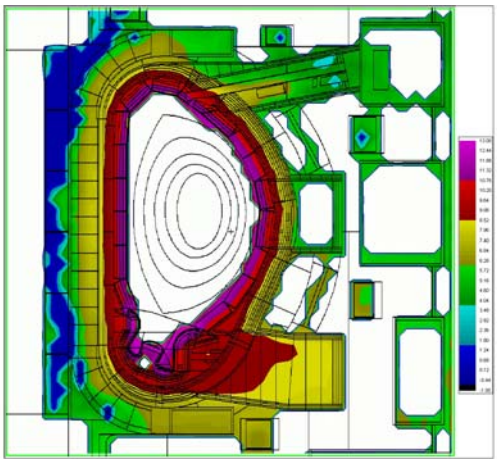

Abb. 2: Geometrie von ITER (rechts)

Da das dort herrschende Neutronen- und Strahlenfeld einen maßgeblichen Einfluss auf Funktion, Materialschäden, Lebensdauer, Abschirmverhalten und Aktivierung der Komponenten hat, ist eine genaue Modellierung und neutronenphysikalische Analyse des gesamten Systems von besonderer Bedeutung. Im Rahmen dieser Arbeit wurde ein detailliertes Modell erstellt, um das Verhalten der Komponenten und Strukturen im Hinblick auf die Neutronenflussverteilung, nukleare Aufheizung und Strahlenschäden zu untersuchen [4].

Simulationsverfahren für die Aktivierungsanalyse

Die Verfahren nutzt die FMESH-Technik von MCNP, wobei ein dreidimensionales Gitter über den zu analysierenden Bereich der Geometrie gelegt wird, welches beliebig in der Größe und Auflösung variieret werden kann. Für jedes Element dieses Gitters wird die Neutronenflussdichte während eines MCNP-Laufs ermittelt und in Form einer zweidimensionalen Matrix ausgegeben, welche zusammen mit dem Geometrie-modell der MCNP-Berechnung dreidimensional (z.B. 3DField) graphisch dargestellt wird (Abb.1 rechts). Die Nutzung der FMESH-Technik für Visualisierungs-zwecke ist besonders hilfreich bei der Darstellung von Daten über das gesamte Geometriemodell und ein effizientes Werkzeug für das Verständnis der unterliegenden physikalischen Prozesse.

Für die Aktivierungsberechnungen mit FISPACT müssen die Ergebnisse von MCNP entsprechend aufbereitet werden. Während letzteres dreidimensionale Verteilungen liefert, erzeugt FISPACT mit der Lösung von Nuklidbilanzgleichungen nulldimensionale Nuklid-vektoren unter Anwendung eigener nuklearer Daten-bibliotheken. Um eine dreidimensionale Aktivitäts-verteilung zu erhalten, werden die MCNP-Daten auf äquidistante Stützstellen bzw. Gitterelemente verteilt, deren Abstände den FMESH-Maschenpunkten entsprechen. Für jedes Gitterelement müssen außerdem noch Materialzusammensetzung und Masse bestimmt werden, was über eine separate Samplingroutine geschieht. Zu diesem Zweck werden mit Hilfe von MCNP zufällige Source-Ereignisse im gesamten Maschennetz generiert, deren relative Häufigkeit in den Elementen den Volumenanteil und die Nuklid-konzentration im jeweiligen Element bestimmt. Diese werden anschließend mit der lokalen Neutronen-flussdichte und dem Spektrum zu einem FISPACT-Inputfile kombiniert.

Die einzelnen FISPACT Ausgabedateien werden wiederum in ein Format umgewandelt, welches verschiedene Größen wie Aktivitätsinventar, nukleare Wärmeleistung und Gammadosis nuklidspezifisch beinhaltet. Diese werden in Verbindung mit dem Geometriemodell zur Visualisierung der Ergebnisse herangezogen. Darüber hinaus wird das von FISPACT erzeugte Gammaspektrum der Aktivierungsprodukte in ein neues Source-File umgewandelt, um damit für dasselbe Geometriemodell und die Konfiguration Gammatransportberechnungen (mit MCNP) durchführen zu können.

Analyse der Rechenergebnisse

Die vorgestellte Schnittstellenroutine wurde mittels existierender MCNP-Modelle für den Kernfusions-reaktor ITER und den CXRS-Port-Plug getestet und geprüft, wobei die früheren, eigenen Berechnungen als auch diese von anderen Forschungsgruppen herangezogen wurden [5][6].

Zu diesem Zweck wurde auf der Basis eines hochaufgelösten MESH-Gitters sowohl für das gesamte ITER-Modell als auch für die ausgewählten Komponenten eine Langzeitsimulation durchgeführt. Die daraus gewonnen Ergebnisse wurden mit Hilfe der hier vorgestellten Schnittstellenroutine für die Aktivierungsanalyse mit FISPACT verwendet. Als Vergleichsgröße wurden das Aktivitätsinventar, die Verteilung der Zerfallsprodukte und Zerfallswärme herangezogen und mit solchen der anderen Gruppen, insbesondere für den CXRS Port Plug verglichen.

An der Position des ersten Spiegels im Labyrinth wurden 7.30E+13 n/cm²s und 1.95 W/cm³ für Neutronenfluss (Abb. 3) bzw. nukleare Wärmeleistung bestimmt. An der Position des hinteren Fensters ergaben sich 4.66E+7 n/cm²s für den Neutronenfluss und 1.20E-6 W/cm³ für die nukleare Aufheizung. Berechnet wurde außerdem die Verteilung der Heliumproduktionsrate an einer kritischen Position an der Vorderseite des Port Plugs. Demnach beträgt das Maximum an dieser Stelle 0.15 ppm, was unterhalb der oberen Grenze von 1 ppm liegt. Die He-Produktionsrate in den geschweißten Bauteilen ist um zwei Größenordnungen geringer als in den umgebenden Komponenten. Der Grund hierfür ist ein höherer Kühlwassergehalt in diesen Strukturen. Der Vergleich mit den Ergebnissen anderer Gruppen zeigt eine Abweichung von weniger als 2 % für den Neutronenfluss und weniger als 10 % für die Heliumkonzentration als Aktivierungsprodukt. Die Abweichungen sind möglicherweise auf die Unterschiede der nuklearen Datenbibliotheken (verschiedene Versionen und Updates) und die statistischen Unsicherheiten des Monte-Carlo-Verfahrens zurückzuführen.

Die Anwendung des neuen Verfahrens auf die komplexe geometrische Struktur und Konfiguration des ITER-Port-Plugs zeigt eine gute Übereinstimmung mit den Ergebnissen anderer Gruppen. Die somit verifizierte Methode bietet ein neuartiges Verfahren zur detaillierten Analyse der neutronenphysikalischen Vorgänge und des nuklearen Materialverhaltens sowohl für die Strukturen des ITER, als auch für jede Anordnung von Materialzellen beliebiger Geometrie. Die darin integrierten Visualisierungsroutinen erlauben die Darstellung physikalischer Vorgänge in hoher Auflösung einerseits und die Untersuchung der Auswirkungen auf die Modell- und Geometrie-variationen andererseits im Hinblick auf die Designoptimierung.

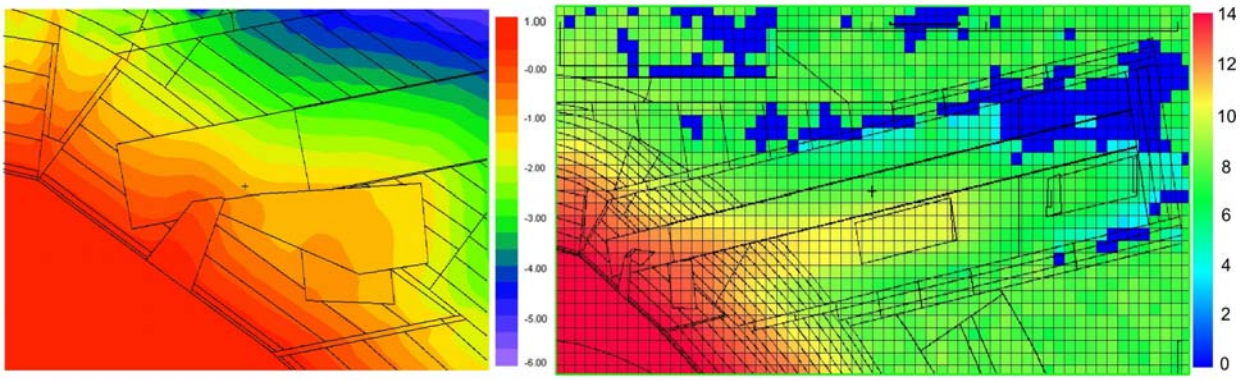

Abb. 3: Ergebnisse der nuklearen Berechnungen für den ITER-CXRS-Port-Plug: Materialschäden [log[dpa]] (links), Neutronenflussdichte [log[1/cm²s]] (rechts)

Referenzen

[1] Briesmeister, J.F.; MCNP5 Monte Carlo N-Particle Transport Code System, RSICC, Los Alamos, 2000, CCC-0730

[2] Forrest, R.A., et al; FISPACT 2005: User Manual, UKAEA Fusion, Report UKAEA FUS 514, 2005

[3] Chen, Y., Fischer, U.; Rigorous MCNP based shutdown dose rate calculations: Computational scheme, verification calculations and application to ITER, Fusion Engineering and Design 63-64 (2002) 107 - 114

[4] Bourauel, P. Nabbi, R.; sophisticated neutronic calculation of the ITER upper port diagnostic system using monte carlo method , RRFM Conference, Hamburg 2008

[5] Shatalov G.E., Sheludikov, S.V.; Upper Port #3 Neutronic Analysis, Moscow 2002, Ref No. G55 MD 161 03-10-06 W 0.1.

[6] Serikov, A, et al; radiation Shielding Analyses for the ITER Upper Port ECRH Launcher; The ANS Topical Meeting of the Radiation Protection and Shielding Division,USA,2007

Monte-Carlo basierte Untersuchungen zum Abbrandverhalten von innovativen Brennstoffen in LWR

O. Schitthelm, R.Nabbi und H.J. Allelein

Institute for Energy Research - Safety Research and Reactor Technology (IEF-6), Forschungszentrum Jülich
Corresponding author: o.schitthelm@fz-juelich.de

Zusammenfassung: Hochaufgelöste Monte-Carlo Simulationen der neutronenphysikalischen Vorgänge in LWR haben gezeigt, dass sich MOX und Thorium basierte Brennstoffe ($(Th/Pu)O_2$) im Bezug auf Neutronenspektrum, Abbrand und Reaktivitätskoeffizienten nicht signifikant unterscheiden. Dies liegt an den ähnlichen neutronenphysikalischen Eigenschaften der Brutstoffe Th-232 und U-238. Im Vergleich dazu zeigt ein auf Molybdän basierender Brennstoff – inert matrix fuel (IMF) – mit PuO_2 als spaltbarem Material ein deutlich härteres Spektrum und damit unterschiedliches Verhalten. Sowohl IMF als auch der thoriumbasierte Brennstoff sind in einigen Aspekten der Plutoniumvernichtung deutlich effizienter als der MOX-Brennstoff. Sie verbrennen aufgrund des fehlenden Brutstoffes U-238 ca. dreimal so viel Plutonium wie MOX und erzeugen dabei weniger höhere Aktiniden wie Americium oder Curium pro umgesetzter Plutoniummasse. Da bei Kernbeladungen mit IMF-Brennstoffen eine hohe Überschusskritikalität entstehen, muss diese durch das Beifügen des abbrennbaren Absorbers Gadoliniumoxid ausgeglichen werden.

Einleitung

In den letzten Jahren sind umfangreiche Forschungsarbeiten durchgeführt worden, um das Abbrand- und Transmutationspotential sowie Sicherheitseigenschaften von IMF und thoriumbasierten Brennstoffen ($(Th/Pu)O_2$) zu untersuchen. Ziel ist es, die Potentiale dieser Brennstoff-Typen im Hinblick auf Reduktion der vorhandenen Plutoniumvorräte zu bewerten [1-3]. Es hat sich gezeigt, dass bei den IMF-Brennstoffen die Verwendung einer metallischen Matrix aus abgereichertem Molybdän eine vielversprechende und realistische Option ist [4]. Im Vergleich zu MOX und klassischen Uranbrennstoffen zeigen sowohl diese IMF-Variante als auch der keramische Thoriumbrennstoff $(Th/Pu)O_2$ neutronenphysikalisch besonders günstige Sicherheitseigenschaften und bemerkenswerte Tranmutations-potentiale für Transurane (TRU).

In der vorliegenden Arbeit wird der Frage nachgegangen, in welchem Ausmaß sich die neutronenphysikalischen Eigenschaften eines LWR-Kerns durch den Wechsel des Brennstoffes von MOX zu $(Th/Pu)O_2$ bzw. IMF verändern. Besonderes Augenmerk wird dabei auf den Brennstoffverbrauch und die Vernichtung von TRU gelegt. Aufgrund der Komplexität der zugrunde liegenden Prozesse sind fortgeschrittene Methoden und hochdimensionale Modelle notwendig. Aus diesem Grund wurde eine paralleliserte Fassung von MONTE-BURNS - basierend auf dem Monte-Carlo Code MCNP und dem Abbrandprogramm ORIGEN – eingesetzt [5,6]. Die hierfür benötigten nuklearen Daten werden mit Hilfe von NJOY generiert [7].

Beschreibung der Brennstoffvarianten

Für die Simulation der physikalischen Vorgänge im Reaktorkern wird von einem Standard 17x17-25 Standard Brennelementen (DWR) mit verschiedenen Brennstoffinhalten ausgegangen. Als erste Variante enthält das MOX-Element eine Mischung aus PuO_2 und UO_2 mit einer Anreicherung von 3.80/0.71 % wt. spaltbarem Plutonium bzw. U-235. Da der IMF-Brennstoff aufgrund des fehlenden Brutstoffes keinen neuen Spaltstoff erzeugt ist eine höhere anfängliche Putoniumanreicherung von 12.8 % wt. mit einem spaltbarem Anteil von 8.6 % wt. notwendig. Der keramische Brennstoff PuO_2 ist dabei in der metallischen Matrix aus abgereichertem Molybdän homogen verteilt. Aufgrund des hohen Gehalts an Pu ergibt sich bei BOL eine hohe Überschussreaktivität, welche mittels des abbrennbaren Absorbers Gadoliniumoxid in ca. einem Drittel der Brennstäbe kompensiert wird. Der thoriumbasierte Brennstoff, $(Th/Pu)O_2$ brütet ähnlich wie MOX neues spaltbares Material, so dass eine vergleichbare Anreicherung von 4.25% wt. spaltbarem Plutonium gewählt wurde. Das Plutonium im IMF Brennstoff stammt aus bestrahltem Uran-Brennstoff mit einem Abbrand von 41 MWd/kgHM. Der Plutoniumgehalt der anderen beiden Brennstoffvarianten ergibt sich aus bestrahlten Uran-Brennstoff mit einem Endabbrand von 33~MWd/kg.

Numerische Methode für die Simulation des Cores

Die komplexe Struktur eines LWR-Kerns erfordert eine präzise Beschreibung der zugrunde liegenden Gometrie. Mit MCNP ist man in der Lage, den Aufbau eines LWR-Kerns von einem einzelnen Brennstab bis hin zu einem Vollcore in hoher Genauigkeit zu und damit core-physikalischen Parameter einschließlich Reaktivitätskoeffizienten zu bestimmen.

Das generierte Rechenmodell bildet dabei die Geometrie der einzelnen Brennelemente durch eine hohe Zahl von Materialzonen ab, wodurch, mit jeder gekoppelter MCNP und Abbrandberechnung (ORIGEN) das neutronenphysikalische Geschehen genau simuliert wird. Dabei sorgt die Interface-Routine MONTE-BURN für

den Datenaustausch zwischen den beiden Programmen und erlaubt eine genaue Erfassung der Nuklidzusammensetzung für MCNP und der kondensierten Wirkungsquerschnitte für ORIGEN.
Um die Berechnungen einheitlich zu gestalten wird von einer einheitlichen Kernbeladung ausgegangen. Dies wird durch reflektierende Randbedingungen an den Grenzen der Brennelementgeometrie erreicht. Das Modell jeder Einheitszelle mit dem Brennstab besteht dabei aus mit Borsäure versetztem Wassermoderator, Cladding, Gasspalt sowie dem homogenen Brennstoff. Für alle Brennelemente bzw. für den gesamten Kern wird eine Leistung von 1000 MW_{th} zu Grunde gelegt, dies entspricht einer Leistung von 17.4 MW_{th} für jedes 17x17-25 Brennelement. Die zeitliche Veränderung der Isotopenzusammensetzung wird mit ORIGEN auf Basis der nuklearen Daten aus den Bibliotheken ENDF/B-VI und VII sowie MCNP-Berechnungen bestimmt.

Ergebnisse

Um die Ergebnisse der Rechnungen vergleichen zu können, wurden sowohl der Thorium- als auch der MOX-Brennstoff 40 MWd/kg abgebrannt. Die daraus resultierende Bestrahlungs- bzw. Betriebsdauer von 800 Tagen wurde für den IMF-Brennstoff zur Erreichung eines vergleichbaren Endabbrandes angewandt. Eine kurze Übersicht des BS-Verbrauches und Pu-Umsatzes wird in Tab. 1 zusammengestellt.

Tab. 1: Ergebnisse Abbrand- und Transmutationsberechnungen für verschiedene Brennstofftypen.

	Unit	MOX	(Th-Pu)-O_2	IMF
Pu initial (total)	kg	25.6	25.0	61.6
Pu Umsatz (total)	kg	7.1	14.9	16.9
Am + Cm production	kg	1.0	1.1	1.7
(Am+Cm) / Pu	%	14.15	7.04	9.89
Pu / Energie	g/MWd	0.38	1.05	1.16

Zum Vergleich ist in Abb.1 das Spektrum im Reaktor mit drei verschiedenen Brennstoff-Beladungen gegeben. Im Vergleich zu den anderen beiden Varianten zeigt der IMF-Kern eine leichte Verschiebung des Spektrums in den epithermischen Bereich, was durch die geringe Resonanzabsorption der Matrix (Mo) in diesem Energiebereich bedingt ist.

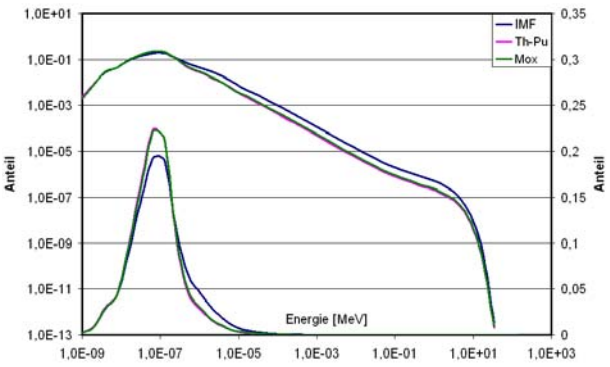

Abb. 1: Neutronenspektrum in LWR-Kern für verschiedene BS-Varianten.

Obwohl der LWR Kern mit dem IMF-Brennstoff einen deutlich höheren anfänglichen Plutoniumgehalt besitzt, setzt er nur geringfügig mehr als beim Thorium-Brennstoff um. Allerdings wird im Kern mit Thorium- bzw. IMF-Brennstoff insgesamt deutlich mehr Plutonium verbraucht als bei der MOX-Variante, da der Beitrag von U-238 zur Bildung neuer Pu und Folgeisotope beträchtlich ist. Die Plutonium-Umsatzrate pro erzeugter Energie ist für die IMF- und thoriumbeladenen Kerne vergleichbar und fast dreimal so hoch wie im MOX-Kern. Wie Abb. 2(a) zeigt, nimmt mit der Bestrahlungsdauer die Umsatzrate im Thorium und MOX-Brennstoff aufgrund des neu erbrüteten Spaltstoffes ab, während sie für den IMF-Kern nahezu konstant bleibt.

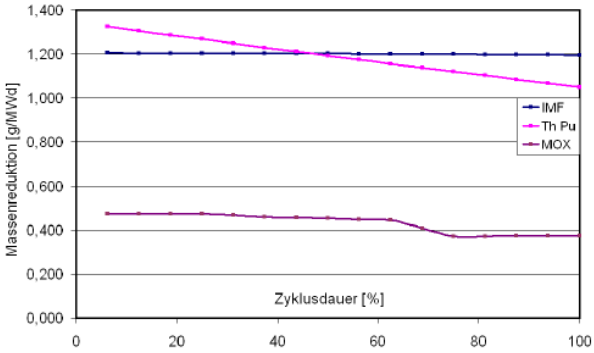

(a) Plutoniumverbrauch

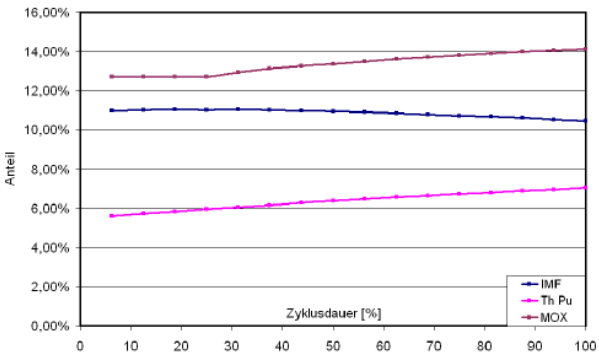

(b) Anteil höherer Isotope

Abb. 2: Zeitliche Veränderung der Plutoniumumsatzraten in Abhängigkeit der Betriebsdauer.

Die Verringerung des Plutoniumbestandes erfolgt hauptsächlich über zwei physikalische Prozesse nämlich Spaltung und Neutronenabsorption, wobei letzterer zur Bildung von höheren Isotopen wie Americium oder Curium führt. Minore Aktinide verursachen im Bezug auf die nukleare Abfallentsorgung ähnliche Probleme wie Plutonium. Aus diesem Grund wird angestrebt, unter maximaler Plutoniumreduktion, den Aufbau höherer Isotope zu minimieren. Wie Abb. 2(b) zeigt, sind diese Anteile für die drei verschiedenen Brennstofftypen unterschiedlich. Die Simulationsergebnisse zeigen, dass der Anteil der Plutoniumvernichtung durch den Aufbau minorer Aktiniden für Thorium- und MOX-Brennstoff mit der Bestrahlungsdauer größer wird, während er für IMF-Kern abnimmt. Allerdings ist insgesamt der Anteil bei dem thoriumbasiertem

Brennstoff auch am Ende der Bestrahlung deutlich geringer als bei IMF-Typ.

Schlussfolgerungen

Das Abbrandverhalten eines Standard-DWR mit innovativen thoriumbasierten Brennstoffen ist vergleichbar mit dem eines mit MOX beladenen Reaktorkerns. Aufgrund des vergleichbaren Plutoniuminhalts und der ähnlichen Eigenschaften der Brutstoffe ergeben sich nur kleinere Unterschiede im Neutronenspektrum. Im Vergleich zu MOX-Cores zeigen Thoriumbrennstoffe allerdings ein deutlich effektiveres Transmutationsverhalten von TRU. Die neue IMF-Variante zeichnet sich durch ein härteres Neutronenspektrum und einen hohen Plutoniumverbrauch aus. Für die Kontrolle der anfänglichen (BOC) Überschussreaktivität ist die Verwendung eines abbrennbaren Absorbers, wie Gadoliniumoxid, erforderlich, dessen Konzentration von der Zusammensetzung des Brennstoffes abhängig ist. Durch die Optimierung der Verteilung des Absorbers wird gleichzeitig eine Glättung der Leistungsdichteverteilung und des Verlaufs der Kritikalität erreicht. Darüber hinaus zeichnet sich der IMF-Brennstoff durch hohe Plutonium-Umsatzrate pro erzeugter Energie bei einer moderaten Rate an erzeugten höheren Aktiniden aus.

Literatur

[1] G. Lombardi, et al, "Neutronic analysis for U-free inert matrix and Thoria fuels for plutonium disposition in PWR", J. Nuclear Materials 274 (1999), p. 181-188

[2] A. Galperin, et al, "Thorium Fuel for Light Water Reactors", Science & Global Security 6 (1997)

[3] T. Bodewich, "Optimized transmutation of Plutonium and Americium in PWR", Report of Research Centre Juelich, Juel-4131 (May 2004)

[4] T.Ogawa, Tulenko, J. Porta,"Innovative fuel forms for better fuel management of nuclear Waste", OECD NEA Workshop on the back end of the fuel cycle, Avignon, France, Oct. 1998

[5] D. I. Posten et al, "Monteburns 2.0: User's Manual", LA-UR-99-4999, (1999)

[6] X-5 Monte-Carlo Team, " MCNP: A General Monte Carlo N-Particle Transport Code, Version 5" LA-UR-03-1987, (2003)

[7] R. Nabbi, et al, "Application of Coupled Monte Carlo and Burnup Method using High Performance Computers", ANS Conf. on MC Methods, Chattanooga, USA (2005)